浊

清

F

Exploring layered double hydroxide efficiency in removal of fluoride ions from water: material insights, synthesis and modification strategies and adsorption mechanisms

Fluoride ion pollution is currently one of the important factors causing chemical risks in drinking water. Adsorption method is an important way to solve this problem due to its simple operation and low cost. Among many adsorbents, layered double hydroxide (LDH) material has the characteristics of simple preparation, adjustable layer composition, adjustable interlayer anion type, and high adsorption capacity. This work provides a comprehensive summary of LDHs used for fluoride ion adsorption, from the perspectives of composition, synthesis, modification, environmental factors affecting adsorption performance, adsorption mechanism, existing problems and future directions.

As featured in:

RSC Sustainability

ROYAL SOCIETY OF CHEMISTRY

rsc.li/rscsus

TUTORIAL REVIEW

Check for updates

Exploring layered double hydroxide efficiency in removal of fluoride ions from water: material insights, synthesis and modification strategies and adsorption mechanisms

Li Sun,[a] Jinan Niu, [iD] *[ab] Hongpeng Liu,[a] Fangfang Liu,[a] Arianit A. Reka,[c] Jakub Matusik [iD] [d] and Peizhong Feng*[ab]

Fluoride ion pollution is currently one of the important factors causing chemical risks in drinking water. The adsorption method is an important way to solve this problem due to its simple operation and low cost. The key to the adsorption method is to develop efficient fluoride ion adsorption materials. Among many adsorbents, layered double hydroxide (LDH) materials have the characteristics of simple preparation, adjustable layer composition, adjustable interlayer anion type, and high adsorption capacity. Thus, they are considered to be highly promising fluoride ion adsorbents. This work provides a comprehensive summary of LDHs used for fluoride ion adsorption, from the perspectives of composition, synthesis, modification, environmental factors affecting adsorption performance, and adsorption mechanisms. Notably, this work distinguishes between LDH and its derivatives such as mixed metal oxides because they have different fluoride adsorption mechanisms. Specifically, the general discussion is focused on the LDH phase, while MMO and complexes are discussed in the modification section. Additionally, problems and future directions in the development of LDH-based fluoride ion adsorbents are explored.

Sustainability spotlight

To ensure the sustainable development of human society, the economy, and the living environment, pollution control of water resources has become a focus of people's attention. Fluoride ions are common harmful ions that pose a serious threat to ecosystems and human health. LDH has a large specific surface area, good ion exchange performance, and high adsorption capacity; therefore, it has promising application prospects in fluoride ion adsorption. The advancement of this work will help reduce the impact of fluorinated wastewater on the environment and ecosystems, protect people's health and maintain ecological balance. At the same time, it will also promote the realization of sustainable consumption and production and contribute to the sustainable development of human society (SDGs 3, 6, and 12).

1   Introduction

Fluorine is one of the essential trace elements for the human body. However, its excessive intake can be harmful to health. For example, long-term intake of low concentration fluoride in the human body will cause dental fluorosis and bone fluorosis, and if the concentration of fluoride is high, it will immediately cause strong stimulation and corrosion of human skin, further leading to dehydration and dissolution of skin tissue protein.[1]

[a]School of Materials Science and Physics, China University of Mining and Technology, Xuzhou 221116, P.R.China. E-mail: jinan.niu@cumt.edu.cn; pzfeng@cumt.edu.cn
[b]Key Laboratory of Coal Processing & Efficient Utilization, Ministry of Education, China University of Mining and Technology, Xuzhou 221116, P.R.China
[c]Faculty of Natural Sciences and Mathematics, University of Tetova, Tetovo 1200, North Macedonia
[d]Faculty of Geology, Geophysics and Environmental Protection, AGH University of Krakow, al. Mickiewicza 30, 30-059 Krakow, Poland

As a result, the World Health Organization (WHO) proposed that the content of fluoride in drinking water should be strictly controlled below 1.5 mg L^{-1}.[2]

The fluoride ion is a major source of fluoride in water. Two main reasons account for the excessive fluoride ion content in drinking water. One is the existence of natural fluoride minerals in the environment, and the other is the discharge of fluoride-containing wastewater from modern industries such as steel metallurgy, aluminum electrolysis, rare earth element separation, photovoltaic cells and semiconductor etching. Due to the huge demand for modern industrial products, the latter type is undoubtedly the main fluoride pollution source in water.

At present, among the methods used to remove fluoride ions from water, ion exchange and reverse osmosis are too expensive to be suitable for large-scale fluoride removal. Electrocoagulation and precipitation methods give rise to still high residual fluoride ion concentration in wastewater, so further processing steps are required, resulting in increased fluoride

removal costs. In comparison, the adsorption method is easy to operate and requires simple equipment, so it has a higher practical value. Consequently, the development of efficient fluoride ion adsorbents becomes the key to solving fluoride ion pollution in water.

Layered double hydroxides (LDHs) have the chemical formula $[M_{1-x}^{2+}M_x^{3+}(OH)_2]_x^+(A^{n-})_{x/n} \cdot mH_2O$ and are also known as hydrotalcite-like materials, where M^{2+} and M^{3+} are divalent and trivalent metal cations, respectively, located in the brucite layer. A^{n-} is the anion located between brucite layers, such as carbonate, nitrate, phosphate, *etc.*; x is the molar ratio of $M^{3+}/(M^{2+} + M^{3+})$; m is the number of water molecules between the sheets. In the LDH structure, the divalent cations form octahedrally coordinated units with six surrounding oxygen. When some divalent cations are partially replaced by trivalent cations, the brucite layer becomes electrically positive. Therefore, negative anions are introduced between layers to maintain electrical balance.[3] Interlayer spacing can be adjusted through anion exchange.[4,5] In addition, the LDH structure has a 'memory effect'; specifically , after LDH is converted into a mixed metal oxide (MMO) along with the removal of interlayer water molecules, anions and hydroxyl groups by thermal activation at 300–500 °C, the LDH structure can be spontaneously restored by exposing the MMO to anionic aqueous solution.[6]

LDH can be either natural or synthetically produced. Natural LDH has low reserves and often contains many impure minerals, so industrial LDH is usually obtained by artificial methods.[7] Compared with other fluoride ion adsorbents such as activated alumina,[8] zeolite,[9] ion exchange resin,[10] and activated carbon,[11] the preparation process of LDH is simple and inexpensive, and its morphology and size can be conveniently adjusted by controlling the type and proportion of introduced metals, which form the layer, to achieve the optimization of fluoride adsorption performance. In addition, the fluoride ion removal capacity of LDH can be further improved by rare element doping, heterocoagulation, anion exchange and thermal activation. All in all, LDH's excellent fluoride adsorption capacity, simple synthesis and flexible performance regulation are becoming more and more valuable in the context of the current tightening environmental pressure and increasing demand for clean drinking water. Therefore, LDH has gained a lot of attention in recent decades. However, there is only one review on LDH for fluoride ion adsorption published by Tajuddin *et al.* in 2023.[12] In their work, the synthesis, characterization, advantages, and composite adsorbents of LDH were reviewed. In addition, conventional defluorination methods, as well as new technologies and new concerns for defluorination in the context of Industrial Revolution 4.0 (IR4.0), were also discussed. However, the modification methods for LDH and the impact of environmental parameters on fluoride adsorption were not included, and there was a lack of statistics and analysis on the adsorption performance of LDH. Therefore, a more comprehensive review is needed to provide an overview of the current state of research progress in LDH fluoride adsorption materials.

Based on this, the research progress since Duan's first report[13] of a LDH-based fluoride adsorbent in 2006 is reviewed
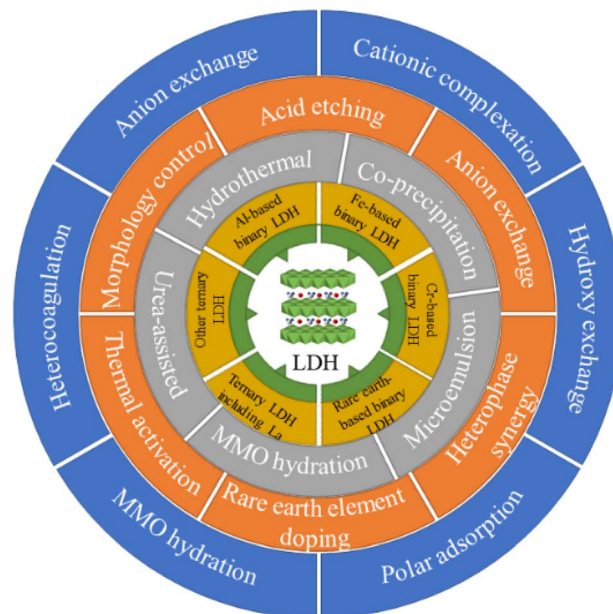
Scheme 1 Categories of LDH fluoride ion adsorbents based on the logical relationship between materials, synthesis, modification and the adsorption mechanism, as indicated in the pie chart from the inside to the outside.

in detail here. First, the types and synthesis methods of LDHs used for fluoride ion adsorption are systematically sorted out, and then the modification procedures of LDHs are classified, including morphology regulation, rare earth element doping, anion exchange, heterocoagulation, and thermal activation. Next, the influencing factors and defluorination mechanism of LDH are discussed. Finally, current problems in LDH research are proposed as well as perspectives on future research. The framework of this review is shown in Scheme 1.

It is worth noting that for a large number of LDH thermal activation studies, fluoride is actually adsorbed by MMO instead of LDH, but most of the publications still use LDH as the title, which brings some ambiguity to the summary of LDH adsorbents. Specifically, for example, when counting LDH synthesis methods, the LDH produced by some synthesis methods is directly used as a fluoride removal agent, while the product obtained by some synthesis is only used as a raw material for MMO, so it is not appropriate to put these two types of LDH synthesis methods together. In order to reduce this confusion, in this work, the main line is based on the phase of LDH, that is, in Sections 2 and 3, the types and synthesis methods of LDH directly used as a fluoride ion adsorbent are counted and classified, corresponding to the performance of the basic structure of LDH. The LDH modification research is reviewed in Section 4, and MMO is introduced as the product of the thermally activated modification of LDH. In Section 4, the morphology control (Section 4.1) is to regulate and modify LDH directly through controlling the synthesis conditions, and it is the original phase of LDH that plays the role of fluoride adsorption; the phase of the adsorbent modified by acid etching (Section 4.2), rare earth element doping (Section 4.3) and anion

Table 1 LDH classification, synthesis, modification and fluoride removal performance statistics

Classification	LDH name	M^{2+}/M^{3+}, $M_A^{2+}/M_B^{2+}/M^{3+}$, M_A^{3+}/M_B^{3+}	Synthesis method	Modification method	Thermodynamic model	Kinetic model	pH at maximum adsorption capacity	Maximum adsorption capacity (mg g^{-1})	Ref
Al-based binary LDH	MgAl-LDH	3:1	Co-precipitation	—	Freundlich	—	5	38.9	41
		2:1	Co-precipitation	—	—	—	6	84	42
		2:1	Co-precipitation	—	Langmuir–Freundlich	—	6	319.80	43
		2:1	Urea-assisted	—	Freundlich	—	7	28.60	44
		2:1	Co-precipitation	—	Langmuir	2nd	7	41.3	45
		2:1	Co-precipitation	—	—	2nd	—	—	46
		2:1	Co-precipitation	—	—	—	—	—	47
		2:1	Co-precipitation	—	Langmuir	2nd	—	62.69	48
		3:1	Co-precipitation	Morphology control	Langmuir	2nd	—	21.72	49
		2:1	Urea-assisted	Morphology control	Freundlich	2nd	6	27.03	50
		2:1	Co-precipitation	Morphology control + thermal activation	Langmuir	—	6	47.70	51
		3:1	Co-precipitation	Morphology control + thermal activation	—	—	—	82.45	52
		4:1	Co-precipitation	Morphology control (various aging treatments)	Redlich–Peterson	2nd	—	44.4	53
		2:1	Co-precipitation	Acid etching	Freundlich	—	3.5	416.67	54
		2:1	Co-precipitation	Heterocoagulation	Temlkin–Phyzev	2nd	5.3~7.1	14.10	55
		3:1	Co-precipitation	Heterocoagulation	Langmuir	2nd	6	2.63	56
		—	Hydrothermal	Heterocoagulation	Langmuir	2nd	5–7	58.70	57
		—	Hydrothermal	Heterocoagulation	Langmuir	2nd	5.71	15.21	58
		2:1	Urea-assisted	Heterocoagulation	—	—	—	—	59
		2:1	Hydro/solvothermal	Heterocoagulation	Freundlich	2nd	5	40.17	60
		5:1	Co-precipitation	Heterocoagulation + thermal activation	Langmuir	—	5	5.03	61
		2:1	Co-precipitation	Heterocoagulation + thermal activation	Langmuir	—	7.5	28.52	62
		3:1	Co-precipitation	Thermal activation	—	—	7	—	63
		2:1	Co-precipitation	Thermal activation	—	—	6	222	42
		2:1	Urea-assisted	Thermal activation	Freundlich	2nd	7	55.22	64
		4:1	Co-precipitation	Thermal activation	Langmuir	2nd	7.2	119.04	65
		2:1	Co-precipitation	Thermal activation	Langmuir	2nd	6	36.86	66
		3:1	Co-precipitation	Thermal activation	Freundlich	—	—	107.60	67
		3:1	Co-precipitation	Thermal activation	Freundlich	2nd	5	91.40	41
		2:1	Co-precipitation	Thermal activation	Freundlich	—	—	213.22	68
		2:1	Urea-assisted	Thermal activation	Freundlich	2nd	6	20.94	13
		3:1	Co-precipitation	Thermal activation	Langmuir	—	—	146.60	69
		2:1	Co-precipitation	—	Freundlich	—	7	247.1	14
	CaAl-LDH	2:1	Co-precipitation	—	—	2nd	6	29.57	70
		1:1	Co-precipitation	—	Langmuir	2nd	6	29.57	71
		3:1	Urea-assisted	Heterocoagulation	Langmuir	2nd	5.87	63.11	72

Table 1 (Contd.)

Classification	LDH name	M^{2+}/M^{3+}, $M_A^{2+}/$ M_B^{2+}/M^{3+}, M_A^{3+}/M_B^{3+}	Synthesis method	Modification method	Thermodynamic model	Kinetic model	pH at maximum adsorption capacity	Maximum adsorption capacity (mg g^{-1})	Ref
		2:1	Co-precipitation	Heterocoagulation	—	—	7	90.00	70
		2:1	Co-precipitation	Thermal activation	—	—	—	59.60	73
		3:1	Co-precipitation	Thermal activation	Freundlich	—	—	108.69	74
		2:1	—	Thermal activation	Freundlich	2nd	8	8.4	75
	CoAl-LDH	1:9	Microemulsion	—	Langmuir	2nd	7	7.13	15
		1:9	Microemulsion	Thermal activation	Langmuir	2nd	7	14.80	15
		2:1	Co-precipitation	—	Langmuir–Freundlich	2nd	10	122.54	76
	NiAl-LDH	2:1	Co-precipitation	Thermal activation	Langmuir–Freundlich	2nd	—	1.20	77
	ZnAl-LDH	1:3	Co-precipitation		Temkin	—	6.4	3.32	78
		1:1	Co-precipitation		Temkin	2nd	6	4.16	79
		1:1	Co-precipitation		—	—	—	25.18	80
		5:2	Urea-assisted	Heterocoagulation	—	—	—	—	81
		2:1	Co-precipitation	Heterocoagulation	—	2nd	6.5	—	16
		2:1	Co-precipitation	Heterocoagulation	Freundlich	2nd	6.4–6.5	8.85	82
		1:1	Co-precipitation	Heterocoagulation		—	—	5.29	81
	LiAl-LDH	1:2	Hydrothermal	Heterocoagulation	Sips	2nd	7.1	62.50	83
		1:2	Co-precipitation	Heterocoagulation	Temkin	—	6.6	—	30
		2:1	Co-precipitation	Thermal activation	Freundlich	2nd	6–7	46.53	17
		3:1	Urea-assisted	Thermal activation	Freundlich	2nd	7	158.70	84
		1:2	Urea-assisted	—	Langmuir	—	7	156.09	85
Fe-based binary LDH	MgFe-LDH	3:1	Co-precipitation	—	Langmuir	2nd	6~7	49.00	86
		3:1	Co-precipitation	Heterocoagulation	Langmuir	2nd	6~7	52.4	86
		3:1	Co-precipitation	Heterocoagulation + thermal activation	Langmuir	1st	7	27.56	87
		2:1	Hydrothermal	Thermal activation	Langmuir	2nd	7	28.65	18
		5:1	Co-precipitation	Thermal activation	Langmuir	2nd	7	50.91	19
	CoFe-LDH	3:1	Co-precipitation	Heterocoagulation	Jovanovich	2nd	7	110.1	88
	CaFe-LDH	10:1	Co-precipitation	Thermal activation	—	2nd	—	463.16	89
	NiFe-LDH	3:1	MMO hydration	Anion exchange	Langmuir	2nd	—	174.68	20
Rare element (RE) binary LDH	MgLa-LDH	—	Urea-assisted	—	Sips	2nd	6	75.97	24
	ZnCe-LDH	1:1	Co-precipitation	Heterocoagulation	Freundlich	2nd	—	167.62	25
Cr-based binary LDH	ZnCr-LDH	3:1	Co-precipitation	—	Langmuir	2nd	—	32.80	22
	MgCr-LDH	3:1	Co-precipitation	—	Langmuir	1st	7	13.16	23
RE ternary LDH	MgFeLa-LDH	3:0.9:0.1	Urea-assisted	Rare earth element doping + thermal activation	Langmuir	2nd	6.8	73.80	28
		3:0.9:0.1	Hydrothermal	Rare earth element doping + thermal activation	Langmuir	2nd	6.8	59.98	29
	MgAlLa-LDH	3:0.9:0.1	Urea-assisted	Rare earth element doping + thermal activation	Sips	2nd	6	51.03	26

Table 1 (*Contd.*)

Classification	LDH name	M^{2+}/M^{3+}, $M_A^{2+}/M_B^{2+}/M^{3+}$, M_A^{3+}/M_B^{3+}	Synthesis method	Modification method	Thermodynamic model	Kinetic model	pH at maximum adsorption capacity	Maximum adsorption capacity (mg g^{-1})	Ref
		3.3 : 1 : 0.1	Co-precipitation	Rare earth element doping + thermal activation	Langmuir	2nd	6	62.33	27
	LiAlLa-LDH	3 : 1 : 0.3	Co-precipitation	Rare earth element doping	Freundlich	2nd	7	46.00	31
		—	Hydrothermal	Rare earth element doping + heterocoagulation	Sips	2nd	7	75.70	90
	NiAlCe-LDH	3 : 0.95 : 0.5	Co-precipitation	Rare earth element doping	Freundlich	2nd	3	238.27	91
Other ternary LDH	MgAlFe-LDH	1 : 0.5 : 0.1	Co-precipitation	Morphology control + heterocoagulation	Langmuir	—	—	—	32
		1 : 0.8 : 0.2	Co-precipitation	Thermal activation	Langmuir	1st	6	14.92	34
		3 : 0.5 : 0.5	Co-precipitation	Thermal activation	Langmuir	2nd	—	42.74	33
		3 : 1 : 0.5	Co-precipitation	Thermal activation	Langmuir	—	4	71.94	35
	CoMgAl-LDH	1 : 2 : 1	Co-precipitation	—	Langmuir	2nd	6	38.01	92
	MgCaAl-LDH	2.5 : 0.5 : 1	Co-precipitation	—	Langmuir	2nd	5	82.35	38
		2.72 : 1 : 0.29	Co-precipitation	Thermal activation	Langmuir	2nd	6	77.9	39
	MgCaFe-LDH	1.25 : 3.75 : 1	Co-precipitation	—	Freundlich	2nd	—	248.44	40
	MgMnAl-LDH	—	Co-precipitation	Thermal activation	Freundlich	2nd	—	58.33	37
	CdNiFe-LDH	0.5 : 3 : 1	Urea-assisted	Heterocoagulation	—	—	—	—	36
	ZnCoCr-LDH	1 : 1 : 2	Hydrothermal	—	Langmuir	2nd	5	108.97	93
	NiMnAl-LDH	2.85 : 0.15 : 1	Co-precipitation	—	Temkin	2nd	5	117.94	94

exchange (Section 4.4) is still LDH, so all of these methods can be classified as intrinsic structural modifications. Meanwhile, the modification using LDH and other substances to perform adsorption at the same time belongs to heterocoagulation (Section 4.5). The adsorption mechanism of thermal activation is substantially different from that of LDH, so it is classified as the last modification method (Section 4.6). In the current classification, the discussion objects of each part of Sections 2–4 (such as different types of LDHs in Section 2, synthetic products in Section 3, and modified products in Section 4) are fluoride ion adsorption materials, instead of precursors or intermediate transition substances. This classification strategy also conforms to the progressive logic from the basic structure and synthesis to performance improvement after modification.

Finally, the three LDH-related terms frequently used in this review are specifically explained: LDH original adsorbent, LDH intrinsic adsorbent and LDH-based adsorbent. The LDH original adsorbent refers to an adsorbent with a basic LDH structure obtained through simple synthesis regulation (corresponding to most LDHs in Sections 3 and 4.1); LDH intrinsic adsorbent means that regardless of the synthesis and modification methods adopted, the LDH structure is finally retained and used for fluoride ion adsorption, so in addition to the LDH original adsorbent, there are also modified products maintaining the phase of LDH (corresponding to most LDHs described in Sections 3 and 4.1–4.4); meanwhile, LDH-based adsorbents generally refer to adsorbents containing LDH or LDH derivative MMO, thus covering the LDH original adsorbent, intrinsic adsorbent and all other modified adsorbents.

2 Types of LDHs used for fluoride ion adsorption

Using different metal ions to synthesize LDH will affect the adsorption of fluoride ions from LDH's intrinsic characteristics. According to the number of metal types found in the structure, LDH used for fluoride ion adsorption can be divided into binary LDH and ternary LDH. Depending on the trivalent metals, binary LDH can be further divided into Al-based, Fe-based, Cr-based and rare earth-based and ternary LDH can be further divided into La-based ternary LDH and other-metal based ternary LDH (Table 1) based on the known studies.

2.1 Binary LDH

2.1.1 Al-based binary LDH. LDH composed of trivalent Al as a metal element and one other monovalent or divalent metal element is currently the most common type of LDH. Among these types of LDHs, MgAl-LDH is the first to be reported for the removal of fluoride ions and is the most widely studied.[13] Compared with other types, it has the advantages of cheap raw materials, large adsorption capacity, and a good fluoride removal effect. In addition to using Mg(II) element with great affinity for F, Ca(II) can also be used to form CaAl-LDH, which can release Ca^{2+} to complex with fluoride ions, thereby increasing the fluoride ion removal capacity. The theoretical

maximum fluoride ion removal capacity of CaAl-LDH can reach 146.6 mg g^{-1}.[14]

CoAl-LDH with interlayer carbonate anions was synthesized by a micro-emulsion method and had a rod-like and hexagonal plate-like mesoporous structure. Although CoAl-LDH has a larger specific surface area, its theoretical maximum fluoride ion removal capacity (14.80 mg g^{-1}) is not very large, possibly due to the low affinity of divalent Co for fluoride ions.[15] A similar behavior has been observed for ZnAl-LDH.[16]

Taking advantage of the fact that the ionic radius of Li$^+$ (0.060 nm) is similar to that of Mg^{2+} (0.065 nm), LiAl-LDH is prepared by using Li$^+$ to replace Mg^{2+} in MgAl-LDH. On the one hand, Li maintains the structural stability of LDH. On the other hand, using monovalent Li ions to replace divalent ions can increase the charge polarity of the LDH layer. Therefore, the electrostatic attraction of the LDH layer to fluoride ions increases, with the theoretical maximum fluoride removal capacity of more than 46.53 mg g^{-1}.[17]

2.1.2 Fe-based binary LDH. Although Al-based LDH has been proven to have good fluoride ion removal ability, the released Al ions will pose certain risks to human health, due to the dissolution of LDH during use at relatively low pH. Therefore, the development of trivalent Al-free LDH becomes a research focus. Fe is widely available and harmless to the human body, so it is naturally used to synthesize Fe-based LDH.

The most studied LDH of this type is MgFe-LDH, which is often synthesized using co-precipitation or hydrothermal methods[18] and modified through interlayer ion exchange, thermal activation, *etc.* to obtain greater fluoride ion removal capacity. However, it is noted that the actual theoretical maximum fluoride ion removal capacity of MgFe-LDH is only 50.91 mg g^{-1},[19] which is far less than that of Al-based LDH, even after modification.

NiFe-LDH with high crystallinity and carbonate anions was synthesized by a high-temperature solvent method, whose ion exchange capacity in the fluoride ion adsorption process can be improved by introducing a high concentration of Cl$^-$ ions to modify the interlayer of LDH. The theoretical maximum adsorption capacity of NiFe-LDH synthesized by this method can reach 174.68 mg g^{-1}, which is significantly higher than that of NiFe-LDH synthesized by traditional methods.[20]

2.1.3 Cr-based binary LDH. The introduction of trivalent chromium into the brucite-like structure has also been one of the directions of LDH research in recent years.[21] Research on Cr-based binary LDH mainly focuses on LDH with intercalated NO^{3-} and Cl$^-$ anions. For example, the NO^{3-} type ZnCr-LDH synthesized by the coprecipitation method has a better fluoride ion removal effect at a molar ratio of 3 : 1 between Zn and Cr than at other ratios; at the same time, it can continuously maintain stable fluoride ion removal capacity in a wide pH range from 3 to 9 with a theoretical maximum removal capacity of 33.00 mg g^{-1}.[22] The fluoride ion removal rates of Cl$^-$ type MgCr-LDH at pH 7 are 88.5% and 77.4%, respectively, when the initial fluoride ion concentrations are 10 mg L^{-1} and 100 mg L^{-1}. The adsorption process is more consistent with pseudo-first-order kinetics and the theoretical maximum removal capacity is 13.16 mg g^{-1}.[23]

2.1.4 Rare earth (RE)-based binary LDH. Rare earth elements have a greater affinity for fluoride ions; therefore, when used as a component of binary LDH, a greater fluoride ion removal capacity can be reached. This type of LDH includes MgLa-LDH[24] and ZnCe-LDH.[25] Using cheap periclase (MgO) and lanthanum salt as raw materials, nano-needle-shaped MgLa-LDH (with carbonate anions) can be prepared through urea assistance and a hydrothermal environment. La enters the hydroxide lattice to replace the divalent Mg cation, making the brucite layer more positively charged. At the same time, more active oxygen is generated in the structure, which tends to be converted into active hydroxyl groups with a higher anion exchange rate in the aqueous solution. Consequently, MgLa-LDH has a high adsorption capacity, and its theoretical maximum adsorption capacity can reach 75.97 mg g^{-1}.[24] In addition, ZnCe-LDH can also be successfully obtained through a traditional co-precipitation method and its maximum adsorption capacity can reach 167.62 mg g^{-1}.[25]

2.2 Ternary LDH

2.2.1 RE based ternary LDH. Although rare earth elements have a high affinity for fluoride, they are very expensive which limits their use for LDH synthesis. One method to overcome this is to add a small amount of rare earth elements to binary LDH, by optimizing the ratio of rare earth elements and other metals to obtain improved cost-effectiveness. The main element added in current research is La. This type of LDH includes MgAlLa-LDH,[26,27] MgFeLa-LDH[28,29] and LiAlLa-LDH.[30,31] In these LDHs, only a small amount of La is needed to achieve high fluoride removal capacity. For example, MgFeLa-LDH with a molar ratio of Mg : Fe : La equal to 3 : 0.9 : 0.1 achieved a high fluoride ion removal capacity.[28,29] Note that not all of these ternary LDHs were used directly as adsorbents; however, most of them were further modified.

2.2.2 Other ternary LDHs. Among many ternary LDHs, in addition to La^{3+}, other common trivalent or divalent metal ions can also be introduced. LDHs containing two trivalent metal elements mainly include MgAlFe-LDH;[32–35] LDHs containing

two elements of divalent metals include CdNiFe-LDH,[36] MgMnAl-LDH,[37] MgCaAl-LDH,[38,39] MgCaFe-LDH,[40] *etc.*

Partial replacement of Al ions with Fe ions at the trivalent metal position is beneficial for the stability of LDH in fluoride ion adsorption and reduces the formation of soluble aluminum fluoride complexes. MgAlFe-LDH synthesized by co-precipitation at a molar ratio of Mg : Al : Fe equal to 3 : 0.5 : 0.5 has an equilibrium fluoride removal capacity of 4.08 mg g^{-1} (12.73 mg g^{-1} after thermal activation) as compared to 2.78 mg g^{-1} observed for MgAl-LDH with a Mg : Al ratio of 3 : 1.[33] LDH containing Ca can achieve efficient fluoride ion removal by releasing Ca^{2+} ions into the solution and then forming CaF precipitate. The theoretical maximum fluoride ion removal capacity of NO^{3-} type MgCaAl-LDH with a molar ratio of Mg : Ca : Al of 1.25 : 3.75 : 1 can reach 248.44 mg g^{-1}.[40]

2.3 Summary

To sum up, LDHs currently used for fluoride ion removal can be divided into two categories: binary and ternary LDHs (Table 1), which can be further subdivided according to the type of trivalent cation. Among binary LDHs, Al-based LDH has the largest number of studies. This is mainly based on the high availability of Al element and the corresponding salts. The fluoride ion removal performance of Al binary LDH is good, but it is noted that their fluoride removal performance has large fluctuations (Fig. 1). LDH in which M^{3+} is Fe^{3+} shows better fluoride ion removal performance, but the number of studies is still small (Fig. 1b). Binary LDHs using other transition elements such as Cr or rare earth elements occupying the M^{3+} position do not show obviously better performance than Al or Fe binary LDH. The following reasons may contribute to the high fluoride adsorption performance of Fe binary LDH: (I) the introduction of iron ions can introduce lattice distortion and change the morphology of LDH, leading to an increase in adsorption sites and a larger specific surface area. (II) The filled 3d orbitals give the iron ions a strong electron transfer capability, which may enhance the electronic interaction between fluoride ions and iron ions, making it easier for fluoride ions to
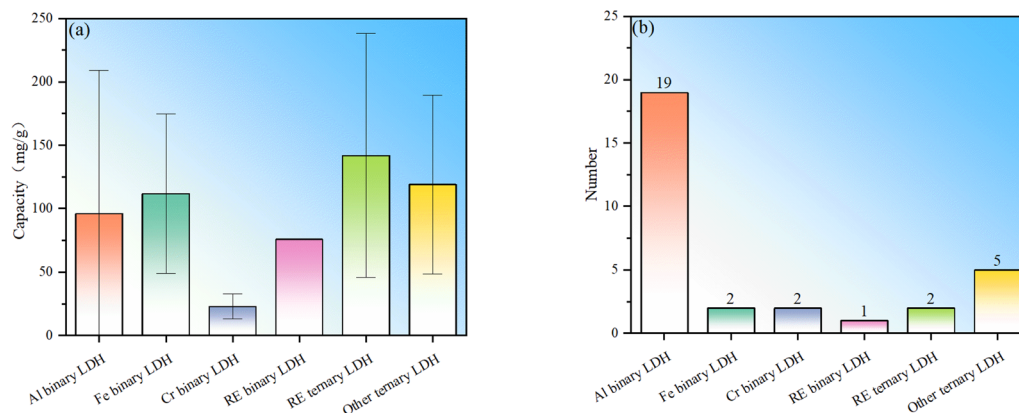

Fig. 1 Statistical histogram of intrinsic LDH fluoride ion removal agents. (a) Removal performance expressed as adsorption capacity and (b) the number of studies (Note: heterocoagulated composites or LDH derivative MMOs are not considered here, and only intrinsic LDH adsorption is compared. There are no error bars for rare element–based binary LDH because of the presence of only one study.).

be adsorbed on the surface of LDH. (III) There may be a synergistic effect between iron ions and other metal ions in iron-containing LDHs, thereby enhancing the overall adsorption capacity of the material.

Trivalent metal-based LDHs have also been synthesized. The composite site where two elements coexist can be a divalent metal site or a trivalent metal site. The composite element can be a common metal or a rare earth metal. La or Ce is found to occupy trivalent metal sites. This type of ternary LDH showed the best average adsorption performance, indicating that the addition of rare earth elements and the synergistic effect of multi-metal components are conducive to performance improvement. Similarly, even ternary LDH without the addition of rare earth elements also showed good fluoride removal performance, further indicating that the synergy of multi-metal components promotes the absorption of fluoride ions.

It should be pointed out that the statistics in Fig. 1 mainly include materials with LDH structures that show fluoride adsorption and do not include samples prepared through the heterocoagulation approach and thermal activation modification. This is mainly to directly compare the differences in the adsorption capabilities of different intrinsic LDHs. In heterocoagulated materials, the contribution of LDH to the overall fluoride ion adsorption performance is difficult to judge. For MMO samples, the fluoride adsorption effect is exclusively caused by the oxide phase, not the LDH phase.

In order to further present to readers the current popularity of various types of LDH in fluoride removal research, further statistics on all LDH-based fluoride removal agents (including heterocoagulated composite and MMO samples) are shown in Fig. 2. It can be seen that Al-based LDH is still the most studied LDH, and it is also found that using conventional metals to prepare ternary LDH-based fluoride adsorbents is relatively hot. Generally, adjusting the type of metal ion, metal ion ratio, defect concentration, particle morphology, interlayer anion

types, *etc.*, can only improve the intrinsic performance to a limited extent, and excessive adjustments may lead to an unstable LDH layer structure. To further improve the fluoride ion adsorption performance of LDH, other modifications may be further supplemented (Section 4).

3 Synthesis

During the formation of LDH, supersaturation is the driving force for LDH nucleation, which is affected by reaction temperature, pH value, composition and proportion of materials, *etc.* In addition, reaction time is also a key factor in determining the kinetics of LDH formation. Therefore, reasonable control of these parameters enables the adjustment of LDH grain size, structure and micromorphology. Currently, hydrothermal, co-precipitation, urea-assisted and MMO hydration methods are found to synthesize related fluoride-removing LDH.

3.1 Hydrothermal

Hydrothermal is a synthesis method that utilizes chemical reactions of substances in solution under certain temperature (≥ 100 °C) and pressure (1–100 MPa) conditions.[95] Sodium hydroxide, ammonia or soda is usually added as an alkali source in LDH synthesis. For example, orderly stacked MgAl-LDH can be synthesized using ammonia as the alkali source and soluble metal nitrate as the metal ion source.[96] When caustic soda was used as the alkali source, the crystallinity of MgAl-LDH gradually improved with the extension of hydrothermal time and the increase of temperature. The obtained particles were oblate and had a narrow particle size distribution, which gradually became larger with the increase of aging time and reaction temperature (Table 2). This can be attributed to the fact that the crystal growth rate is proportional to the reaction temperature.[97]

Insoluble oxides can also be used as metal ion sources to synthesize LDH. Using MgO and Al_2O_3 as raw materials, MgAl-LDH was synthesized through hydrolysis and precipitation of oxides under high temperature and high pressure conditions without adding other alkali sources;[98] meanwhile, by adding NaCl, $NaHCO_3$ or Na_2CO_3 during the synthesis, MgAl-LDH with Cl^- or CO_3^{2-} as the interlayer anion can be obtained.[99] However, it is noted that there are relatively few studies on the synthesis of LDH adsorbents through high-temperature hydrothermal using insoluble oxides or hydroxides as raw materials, due to the low efficiency of the reaction.

3.2 Co-precipitation

Co-precipitation is the most common method for preparing LDH materials, by mixing divalent and trivalent metal salt solutions in a certain ratio, and adjusting the pH of the solution to reach supersaturated conditions to produce metal hydroxide precipitation.[100] The co-precipitation method is divided into low saturation and high saturation co-precipitation. In the low-saturation co-precipitation method, the metal salt mixed solution is slowly added to the separate aqueous solution, and at the same time, the alkaline solution is added dropwise to maintain
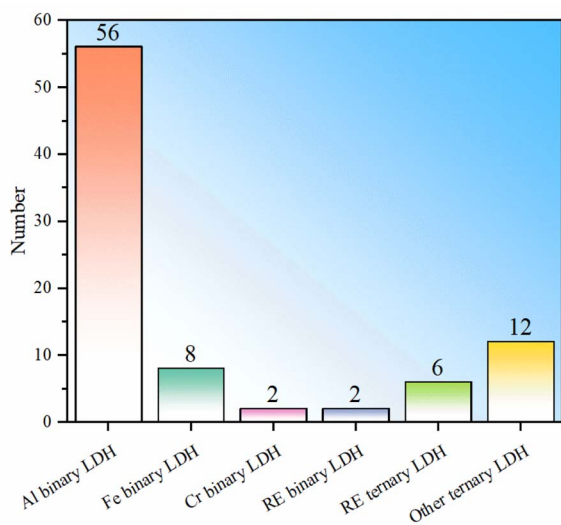

Fig. 2 Statistical histogram of the number of research studies on LDH-based fluoride removers (including heterocoagulated composites and MMO derived from LDH).

Table 2 Effects of aging time, reaction temperature, and total metal ion concentration on LDH particle size[97]

Synthesis method	Aging time (h)	Temperature (°C)	Total metal concentration (M)	Particle size (nm)	Standard deviation (nm)
Hydrothermal	12	100	0.133	85	14
	24	100	0.133	100	15
	48	100	0.133	115	13
	72	100	0.133	120	23
	48	100	0.133	115	13
	48	125	0.133	210	28
	48	150	0.133	290	56
	48	180	0.133	340	29
Urea-assisted	6	90	0.6	860	490
	30	90	0.6	1930	330
	45	90	0.6	2140	240
	69	90	0.6	2200	300
	672	65	0.87	1170	220
	672	65	0.65	2140	330
	672	65	0.44	2740	790
	672	65	0.065	4470	420

the pH required for co-precipitation, while in high-saturation co-precipitation, the metal salt mixed solution is added directly to the alkaline solution. Since the latter approach results in relatively low crystallinity and the formation of other metal hydroxide impurities, further thermal treatment is often required.[101] In general, co-precipitation is a reliable, simple and low-cost way to synthesize most types of LDH materials.

LiAl-LDH synthesized by the co-precipitation method has smaller particles than LDH synthesized by the urea method and has a highly crystalline and ordered layered structure. The maximum adsorption capacity of fluoride ions can reach 46.53 mg g^{-1}.[17] Note that in current research, LDH synthesized by the co-precipitation method is mostly used as the basis before further modification; for example, MgAl-LDH synthesized by the co-precipitation method was used to produce MMO with 82.3% fluoride removal capacity at pH = 7 and an initial fluoride ion concentration of 5 mg L^{-1}.[63]

3.3 Urea-assisted method

Essentially, the urea-assisted method is a type of co-precipitation method, but due to its stable pH control and frequent use, it is classified separately here. Compared with the hydrothermal method, which uses caustic soda, ammonia or soda to provide an alkali source, this method mainly decomposes urea to produce ammonia (reaction eqn (1)) to control the pH of solution:

$$CO(NH_2)^{2+} + 2H_2O = CO_3^{2-} + 2NH_4^+ \qquad (1)$$
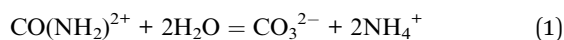
Since the decomposition rate of urea can be controlled through the reaction temperature, the particle size distribution of LDH can therefore be controlled.[102] However, because the urea method is usually performed slightly above room temperature, the LDH nucleation rate is low and eventually larger particles are formed compared to other methods (Table 1).[97] This method can be used for the purposeful synthesis of large-sized, well-shaped LDH.[84,103]

Most of the research on using the urea-assisted method to synthesize LDH for fluoride adsorption uses a reaction temperature above 100 °C to increase the decomposition rate of urea and thus the nucleation rate of LDH.[104] In addition, since urea can produce carbonate ions during the decomposition process, the method mainly synthesizes carbonate intercalated LDH. The presence of carbonate is not conducive to the adsorption of fluoride ions, so further modification is usually required.

3.4 Microemulsion

Microemulsion is a thermodynamically stable dispersion system formed by two incompatible liquids with the assistance of surfactants. It is divided into water-in-oil microemulsion (w/o) and oil-in-water microemulsion (o/w). The particle size of microemulsion droplets is 5 to 70 nm, and the internal space can be used as a microreactor. Particle growth ends when the reactants are consumed. Therefore, microemulsion can control the size of nanoparticles without the use of expensive equipment. Microemulsion is an important approach for preparing monodisperse nanoparticles, which has been greatly developed and improved in recent years. For example, a mixed nitrate solution of Co and Al was used as the water phase and aviation kerosene was used as the oil phase to form a microemulsion. Then ammonium bicarbonate solution was added to provide an alkaline environment, and the reaction was carried out under high temperature and high pressure conditions. Finally, rod-shaped and hexagonal plate-shaped CoAl-LDH was synthesized.[15]

3.5 MMO hydration

The "memory effect" of LDH can be used to rehydrate (reconstruct) the layered structure. The calcination of (thermal activation) will gradually remove the interlayer structural water, anions and hydroxyl groups, thereby leading to MMO; when MMO is dispersed in an aqueous solution with anions, MMO

can be rehydrated and the LDH layered structure is restored; at the same time, the interlayer space is filled with hydrated anions from the solution. It was noted that MMO is hydrated while adsorbing fluoride ions. The adsorption process essentially reflects the fluoride ion adsorption capacity of MMO, rather than that of LDH obtained after MMO hydration. At present, the only relevant study on the preparation of defluorination agents from LDH after MMO hydration is to soak the oxide precursor $(NaNi_{0.75}Fe_{0.25}O_2)$ prepared by a high-temperature flux method in ultrapure water for topological orientation transformation.[20] The cationic valence state of the oxide layer changes from Ni^{3+} to Ni^{2+}, and carbonate (CO_3^{2-}) and water molecules are embedded between the layers at the same time. However, the LDH product was not directly used as an adsorbent in the study, but was further modified by anion exchange (Section 4.4).

3.6 Summary

To sum up, there are currently five main types of synthesis methods for LDH fluoride ion scavengers: hydrothermal, co-precipitation, urea-assisted, microemulsion and MMO hydration (Fig. 3). The samples prepared by the hydrothermal method appear to have the best performance, but the number used directly as defluoridation agents is relatively small and the statistics are weak. The average performance of samples synthesized by the co-precipitation method is the second best, but the number of studies is the largest (Fig. 3). The performance of samples obtained by the urea-assisted method is not as good as that of the co-precipitation method. The reason may be that the LDH particles synthesized by co-precipitation are smaller, while the size of LDH synthesized by the urea method is larger. In addition, the urea method will decompose to produce carbonate ions during the synthesis process, which further hinders the exchange and adsorption capacity of fluoride ions. Nevertheless, we must point out that the urea-assisted method has certain advantages in synthesizing LDH with regular shapes. The adsorption capacity of LDH synthesized by

microemulsion is relatively low, which may be determined by the properties of the material itself in the example. This method can be used to synthesize other LDH materials for further testing. Regarding the hydrothermal and MMO hydration methods, no direct synthesis of LDH for fluoride ion adsorption has been found so far. The reason may be that hydrothermal has higher requirements for production equipment and processes. Although LDH obtained by rehydrating MMO is theoretically feasible, its practical value is not big.

To further demonstrate the research popularity of various synthesis methods for LDH-based fluoride ion adsorbents, the synthesis methods corresponding to all LDH-based fluoride adsorbents (including heterocoagulated and MMO samples) are also statistically analysed (Fig. 4). It can be seen that for the preparation of LDH-derived fluoride ion adsorbents, co-precipitation is still the most commonly used, proving the convenience of such synthesis. The urea-assisted and hydrothermal methods, which are similar to the co-precipitation
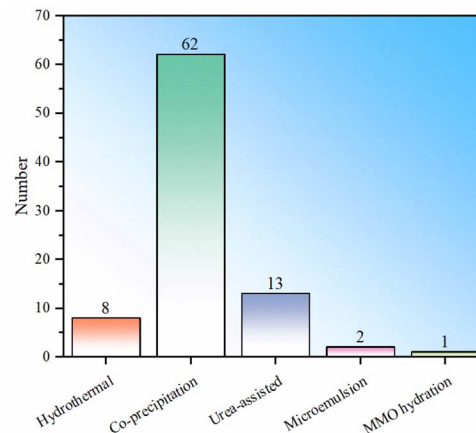
Fig. 4 Statistical histogram of LDH synthesis methods for LDH-related fluoride adsorbents (note: including heterocoagulated or hydrotalcite derivative MMO samples).
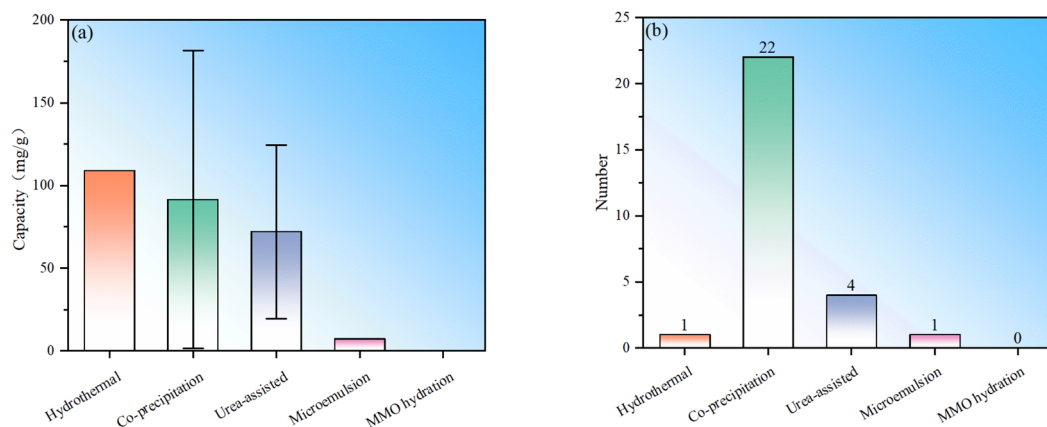
Fig. 3 Statistical histogram of the synthesis of the LDH original fluoride adsorbent. (a) Fluoride ion removal performance corresponding to different synthesis methods, (b) the number of studies corresponding to different synthesis methods (only the basic LDH phase obtained by adjusting synthesis conditions in Sections 3 and 4.1 is counted. There is only one study on hydrothermal and microemulsion, respectively, so there is no error bar for them).

method, are also relatively widely used. The MMO hydration method has been rarely studied to synthesize MMO fluoride removal material precursors, indicating that this method may not have advantages in synthesizing fluoride ion adsorbents. In addition, microemulsion has also been investigated to synthesize MMO precursors, but the number of studies is currently sparse.

4. Modification

In order to increase LDH's fluoride ion removal efficiency, the LDH material is usually further modified through morphology control, acid etching, rare earth element doping, anion exchange, heterocoagulation and thermal activation. The first four modifications do not destroy the basic brucite-like layer of LDH; heterocoagulation involves mixing LDH with other phases to achieve co-adsorption or additional properties, while thermal activation transforms the brucite-like layer into a mixed oxide structure.

4.1 Morphology control

By adjusting process parameters, LDH materials can have various morphologies and produce high-density adsorption sites, which help to improve the fluoride ion removal performance. For example, a shorter hydrothermal aging time can be used to obtain MgAl-LDH with a larger specific surface area, while a longer hydrothermal aging time will lead to the emergence of the $Al(OH)_3$ phase and reduce the specific surface area.[50] The use of starch in the synthesis of MgAl-LDH can stabilize the micromorphology and form particles with a smaller particle size and narrower distribution, thus significantly improving the fluoride ion removal performance.[49] It can be found that the LDH obtained by liquid nitrogen drying had a lower crystallinity and was composed of fine agglomerated nanoparticles, so its adsorption performance was significantly improved compared to that of the sample dried in an oven at 100 °C.[52]

Some studies pointed out that the morphology of LDH basically remains unchanged after thermal activation.[84] Therefore, the morphology of MMO can be controlled by controlling the synthesis conditions of LDH. In other words, the morphology changes of MMO reflect the effect of the control conditions on the morphology of LDH. By changing the molar ratio of metal ions $(Li^+/Al^{3+} = 2, 3, 4, 5)$, the morphology of Li/Al-MMO can gradually evolve from hexagonal nanosheets to petal-like combinations to interconnected petal-like structures.[84] The

crystallinity of the MgAl-LDH material can be adjusted by controlling the amount of doped La, and finally rice-like nano-Mg/Al/La-MMO nanoparticles are formed.[26] The particle size of MgAl-LDH prepared using co-precipitation assisted ultrasound is smaller (80 mm) than that prepared by the traditional co-precipitation method (120 nm).[51]

4.2 Acid etching

Acid etching treatment of LDH will partially dissolve and release metal elements and protonate the LDH surface, and thus the LDH surface can be activated. If an appropriate acid type is selected, the interlayer anions will be exchanged for acid ions that facilitate the next exchange with fluoride ions. For example, since the affinity of LDH for carbonate is much greater than that of fluoride ions, the presence of interlayer carbonate is not conducive to the adsorption of fluoride ions. Consequently, the reduction of interlayer carbonate and the replacement of carbonate by other acid ions can improve the subsequent fluoride ion exchange. In addition, the hydrogen ions in the acidification process may react with the intercalated carbonate ions to form CO_2, which is later released, by following eqn (2):[105]

$$CO_3^{2-} + 2H^+ \rightarrow H_2CO_3 \rightarrow H_2O + CO_2 \tag{2}$$
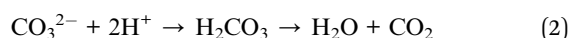
During acidification with hydrochloric acid or formic acid, carbonate ions between the layers were partially or completely removed, and Cl or formate ions were introduced between the layers, which are easily replaced by F^- ions. So, the fluoride ion adsorption performance of MgAl-LDH was significantly improved after acid etching (Table 3).

Note that moderate acid etching can replace interlayer anions while forming a large number of interlayer active sites, which is beneficial for further improvement of fluoride ion adsorption capacity. However, if the etching is excessive, it may destroy the LDH structure and damage the fluoride ion adsorption performance and may also release a large amount of easily soluble elements, such as Al, Mg, *etc.*, which may cause secondary pollution (Table 3).[54] However, there is no relevant research on the correlation between interlayer anion replacement and metal cation dissolution in the acid etching process.

4.3 Rare earth element doping

Rare earth elements are considered to have the effect of improving the structure of the adsorbent, because they can provide more active sites for complexation or ligand exchange with fluoride. At present, most research is done on La element

Table 3 The number of fluoride ions adsorbed by LDH after acid etching and the concentration of Al and Mg in the solution on after LDH activation.[54] Copyright 2011, American Chemical Society

| Adsorbent	Qe (mg g^{-1})	Al (mg L^{-1})	Mg (mg L^{-1})
MgAl-LDH	39.48	—	—
MgAl-LDH etched with 0.1 mol per L HCl	174.50	846.8	717.3
MgAl-LDH etched with 0.1 mol per L HCOOH	176.00	438.0	1375.3
MgAl-LDH etched with 0.01 mol per L HCOOH	83.08	48.5	250.5

doping. For example, after LiAl-LDH was doped with La, it had high fluoride ion adsorption performance in a wide pH range of 5–9. The fluoride removal kinetic curve conformed to the pseudo-second-order equation and the equilibrium Freundlich model. The maximum adsorption capacity is twice that of LiAl-LDH, and 7 times that of activated alumina, which can be attributed to the addition of La increasing the number of active sites that fluoride ions can bind to.[31]

Doping La during the preparation of MgAl-LDH can produce a three-dimensional rice-like micromorphology.[26] La not only adsorbs fluoride through interlayer adsorption and ligand exchange, but also serves as a structure inducer to adjust the crystallinity of the material.[26] In addition, some studies have shown that doped La can increase certain distortion of the LDH structure, which influences the surface morphology and structure of LDH.[27,29,90]

4.4 Anion exchange

A distinctive feature of LDH is its high anion exchange capacity, which mainly depends on the type of anion used when the LDH sheet composition is fixed. The affinity order of LDH sheets for different common anions is as follows:

$$NO_3^- < Br^- < Cl^- < F^- < OH^- < SO_4^{2-} < CO_3^{2-}$$
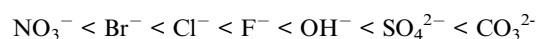
It can be seen that LDH has the greatest affinity for carbonate and sulfate anions, so when these anions dominate, it becomes difficult for fluoride ions to be adsorbed through ion exchange. The affinity of LDH for NO_3^-[107] and Cl^- is weaker than to fluoride ions, so these two types of anions can be used to modify LDH by interlayer exchange and then adsorb fluoride ions.

NiFe-LDH with carbonate ions is first prepared through NiFe-MMO hydration, and then Cl^- ions are used to replace CO_3^{2-} ions to obtain a NiFe-LDH(Cl) adsorbent (Fig. 5). It has high crystallinity, porosity and a unique particle shape, with the highest F^- adsorption capacity of 176.15 mg g^{-1}.[20]

NO_3^- and Cl^- anion modified LDHs have significant fluoride removal effects, and the pH of the solution after the fluoride removal will not increase obviously. However, it should be pointed out that because CO_3^{2-} ion contamination is prone to occur under conventional synthesis conditions, the regeneration conditions for this strategy need to be strictly controlled and are relatively cumbersome.

4.5 Heterocoagulation

Although the aforementioned intrinsic modification methods such as morphology adjustment, acid etching, doping, substitution and other intrinsic modification methods can significantly improve the fluoride ion adsorption performance of LDHs, in many cases the nature of the material itself limits further improvement. Moreover, taking into account the growing multifunctional needs of industry, other possibilities must be explored. Such an approach involves compounding LDH with other materials. Materials compounded with LDH can mainly include organic materials, such as polystyrene,[83] thermoplastic polysulfone,[70] polyethersulfone,[30,56] cellulose,[25,72] chitosan,[61,87] etc.; carbon materials such as biochar[39] and graphene;[81] metal-bearing materials such as aluminum foam; metal oxides such as magnetic iron oxide,[59,62] Al$_2$O$_3$,[16,57] and CeO$_2$;[86] and other materials such as natural sand,[55] etc.

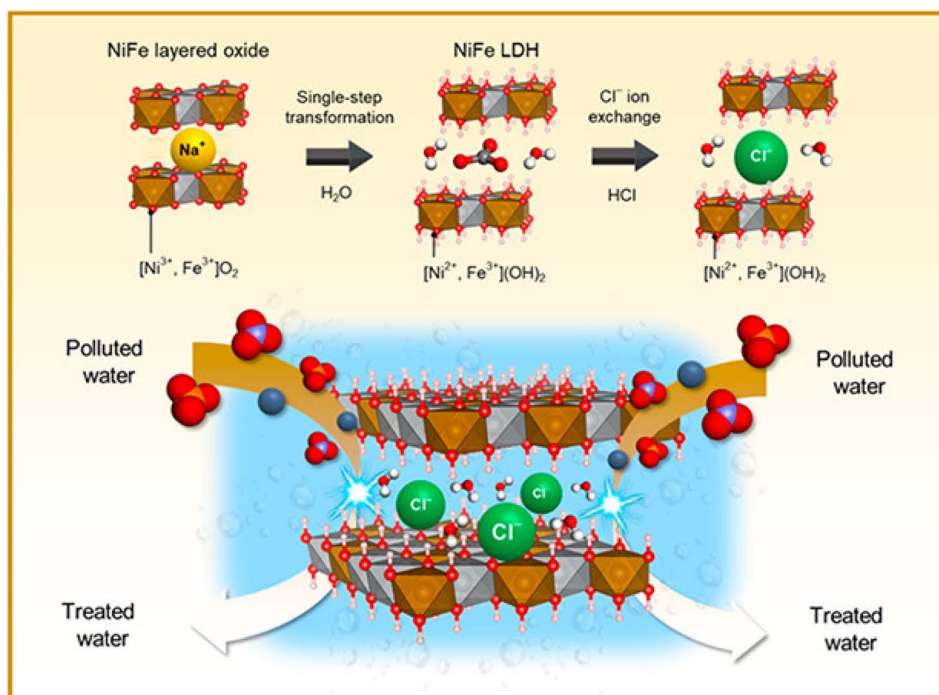When LDH is compounded with heterophases, some LDH with small particle size is often loaded on some larger matrix

Fig. 5 Schematic diagram of the synthesis of NiFe–LDH with interlayer Cl ions.[20] Copyright 2021, American Chemical Society.

materials, so that LDH nanoparticles are less likely to aggregate. Thus, the active sites are then exposed to a greater extent, and at the same time, their recycling is facilitated. For example, LiAl-LDH is loaded on a commercial polystyrene anion exchanger. LDH particles are dispersed in the pores of polystyrene, improving their dispersion. At the same time, this compounding improves the chemical and mechanical stability of the composite, allowing it to be applied in a wide pH range from 3.5 to 12.[79] Organic materials with excellent fluoride ion adsorption properties can also be combined with LDH to form materials of high synergy for the removal of F^-. For example, if a cellulose material rich in hydroxyl groups was used to composite with CaAl-LDH, the theoretical maximum adsorption capacity reached 63.1 mg g^{-1}, which is significantly higher compared with pure cellulose and raw LDH; the fluoride removal mechanism is mainly chemical adsorption, which is consistent with the Langmuir model, indicating that significant hydroxyl displacement adsorption occurred.[72,80]

4.6 Thermal activation

Converting LDH into MMO through thermal activation can improve the fluoride removal capacity of LDH materials. There are three reasons behind this phenomenon: firstly, the thermal activation can remove intercalated carbonate ions; secondly, the dehydroxylation of LDH leads to the formation of mesopores and an increase in the specific surface area, thereby increasing the number of adsorption sites;[108] and thirdly, during the hydration reconstruction process, fluoride ions can be attracted into the LDH layer as charge compensating ions, so the fluoride ion adsorption capacity is high by taking advantage of the "memory effect".[109]

The thermal activation temperature can have a significant impact on the LDH fluoride removal performance (Fig. 6). For example, as the thermal activation temperature of MgAl-LDH increased, the crystallinity of MgO in the product gradually increased; when the temperature was too high, the layer structure would not be destroyed and the MgAl$_2$O$_4$ spinel phase was generated. Although the specific surface area increased, the spinel phase could not be transformed into the LDH structure through the memory effect, so it hampered the fixation of fluoride ions.[67,110] However, when the thermal activation temperature was too low, carbonate ions remained between the layers, and the brucite layer was insufficiently activated, which would also lead to poor fluoride ion adsorption performance. Therefore, it is crucial to optimize the LDH activation temperature to achieve satisfactory fluoride ion removal performance.

It is generally believed that most LDHs have memory effects. However, when comparing the structural changes after the calcination of MgAl-LDH, NiAl-LDH and CoAl-LDH, only MgAl-MMO could be restored to the MgAl-LDH structure after being exposed to aqueous fluoride ions, whereas the other types of MMOs did not show a similar behavior.[80,111]

Compounding pretreatment of LDH can improve the subsequent MMO morphology and fluoride ion adsorption capacity. For example, MgFe-LDH loaded on chitosan prepared by the co-precipitation method had a specific surface area of about 16.38 m^2 g^{-1} before activation, while the specific surface area after thermal activation was 116.98 m^2 g^{-1} with a theoretical maximum fluoride removal capacity of 27.56 mg g^{-1}, mainly because the dispersion of carbon inhibited the aggregation of MMO.[87]

A core/shell/shell mesoporous MgAl-LDH composite was synthesized with magnetic Fe$_3$O$_4$ microspheres as the core, SiO$_2$
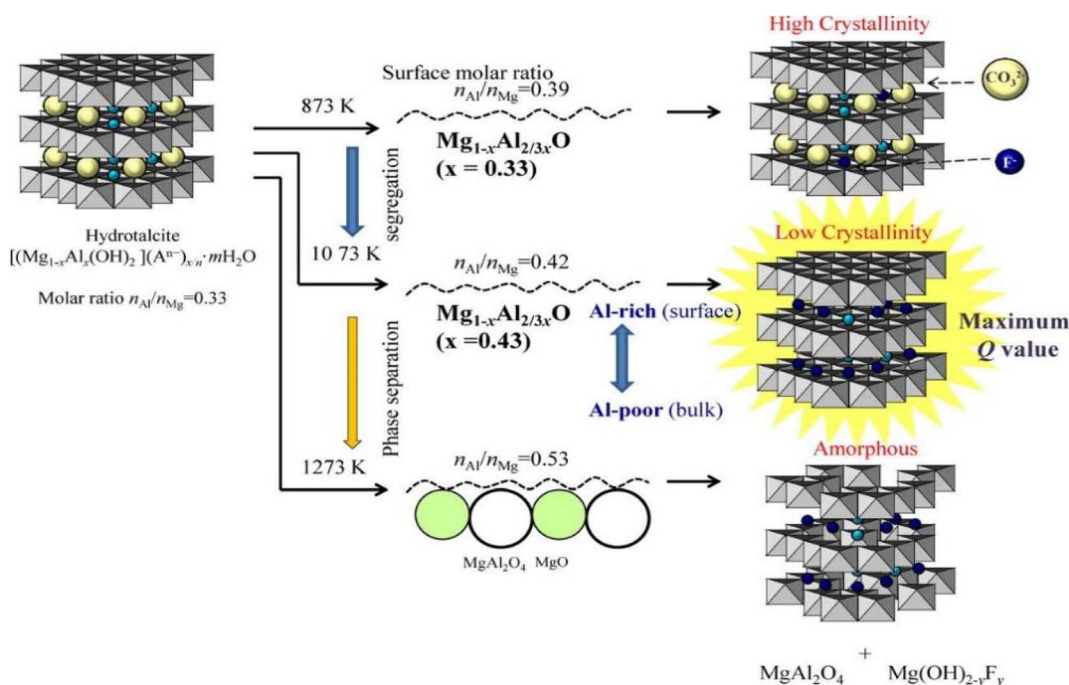

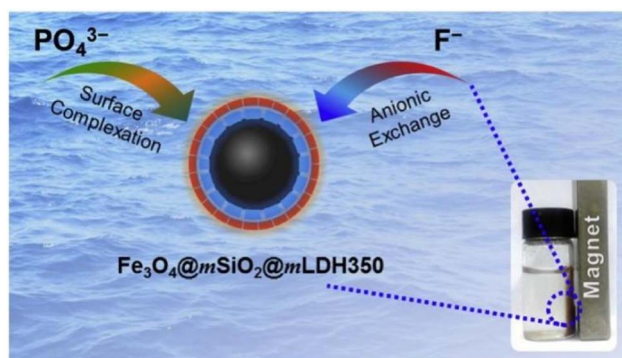Fig. 6 Effect of calcination temperatures on the structure of LDH.[67] Copyright 2014, Elsevier.

Fig. 7 Fe$_3$O$_4$@mSiO$_2$@mLDH350 composite adsorbent.[57] Copyright 2020, Elsevier.

as the inner layer, and MgAl-LDH as the outer layer. It had a large specific surface area and a good mesoporous structure with a theoretical maximum fluoride ion removal capacity of 28.51 mg g^{-1} after thermal activation at 350 °C (Fig. 7).[62]

4.7 Summary

In summary, in order to improve the fluoride ion removal ability, LDH can be modified via morphology control, acid etching, rare earth element doping, anion exchange, heterocoagulation and thermal activation. Statistics were conducted on the fluoride ion removal effects of each modification method, and it is observed that although morphology control modification is the simplest, the fluoride ion removal is generally weak (Fig. 8). By compounding LDH with other materials, the fluoride ion removal capacity is not significantly improved, but the composite adsorbent can have properties that the LDH component does not have, expanding the application fields of LDH. The fluoride removal performance derived from the rare earth element doping method is significantly improved compared to morphology control, indicating the great potential of this method. Anion exchange modification has a more obvious improvement effect than RE doping and heterocoagulation, but the number of studies is

small, which may be due to the difficulty of anion exchange. There are many studies on thermal activation modification, and the fluoride ion removal effect is also more obvious than that of morphology control. However, thermal activation needs to be carried out at high temperature and consumes more energy. In addition, it is noted that the fluoride ion removal ability of thermal activation modification has a wide range, mainly because the fluoride ion removal performance is not only related to the modification method, but also related to the structure and morphology of starting LDH.

Statistics on the number of modifications among LDH-based fluoride ion adsorbents were conducted (Fig. 9). It can be seen that the distribution of the number of studies involving multiple modifications is the same as that of single modification, and the thermal activation method is still the most studied, which once again shows that the thermal activation process is easy to implement. Compounding modification is also widely studied, mainly due to people's expectations for performance expansion and improvement by other "good" materials that have
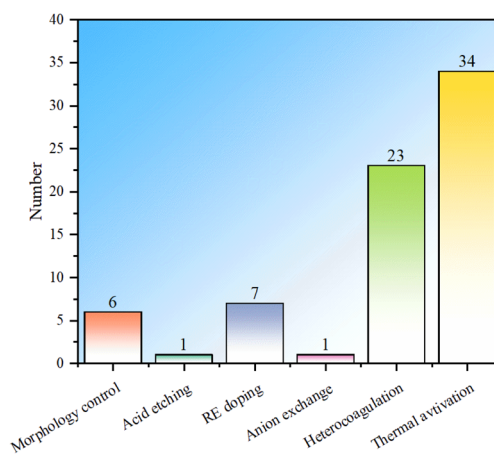

Fig. 9 Statistical histogram of the number of studies on modification of LDH-based adsorbents (all LDH-based adsorbents including heterocoagulated or MMO samples).
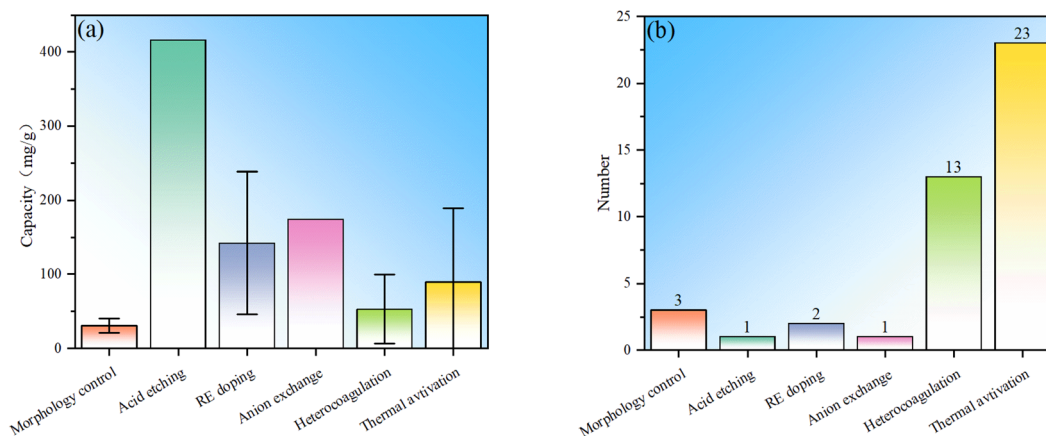

Fig. 8 Statistical histogram of the single modification method of LDHs. (a) Fluoride removal performance corresponding to different modification methods and (b) the number of studies corresponding to different modification methods (only LDHs with a single modification are counted. There is only one study on acid etching, anion exchange modification and rare earth element doping, respectively, so error bars are not included).
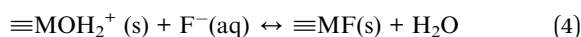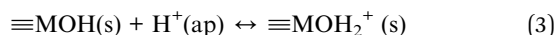
advantages in certain aspects. There are only a few studies on morphology control, indicating that the modification effects of these conventional methods are limited, while there are only a few studies on acid etching and anion exchange, indicating that these methods may have some limitations. This result well demonstrates the popularity of various modification methods in the research of LDH-based fluoride ion adsorbents.

5. Factors affecting fluoride ion adsorption

The adsorption of fluoride ions by LDH and its derivative MMO will be affected by several factors such as pH, temperature, adsorbent dose or competitive effect of coexisting anions. This section summarizes the general rules regarding these influencing factors. It should be noted that after analyzing existing research results, it was found that the impact of environmental factors on most LDHs and MMOs has roughly the same trend, so they are discussed together here.

5.1 pH

The effect of pH on the adsorption of fluoride ions is mainly through its effect on the surface charge of LDH. Generally speaking, as the pH decreases, the fluoride ion removal ability of LDH increases (Fig. 10).[75,112] This phenomenon is similar to that of some other adsorbents such as alumina, hydroxyapatite, and activated carbon. This can be explained by the fact that when pH < pH_{pzc} (pH at zero point potential), the surface of LDH is protonated, resulting in a positive charge on the surface, which is conducive to the adsorption of fluoride ions through electrostatic interaction. This process can be expressed as shown in eqn (3) and (4).

$$\equiv MOH(s) + H^+(ap) \leftrightarrow \equiv MOH_2^+ (s) \tag{3}$$

$$\equiv MOH_2^+ (s) + F^-(aq) \leftrightarrow \equiv MF(s) + H_2O \tag{4}$$

Low pH may also lead to structure dissolution and release of metal ions, which leads to the formation of precipitates if the corresponding fluoride or anionic salt is insoluble. For example,
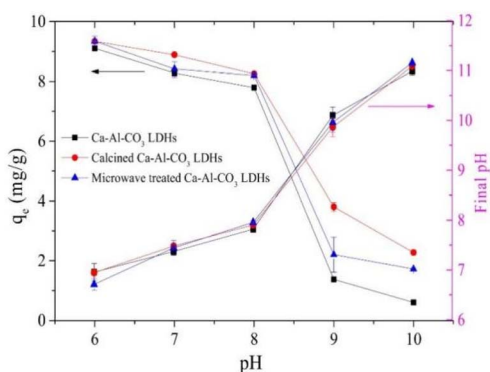
LaFeMg-LDH will release La and Mg under acidic conditions and complex with fluoride ions to form a precipitate.[24] However, too low pH may destroy the LDH structure, thereby reducing the fluoride ion adsorption efficiency.

When pH > pH_{pzc}, hydroxylation (deprotonation) occurs on the surface of LDH, so the negative charge density increases, which is not conducive to the adsorption of fluoride ions through electrostatic force; in addition, a high concentration of hydroxides in the solution will lead to competition with fluoride ions for adsorption sites, which will subsequently reduce the adsorption of fluoride ions. For example, when the ambient pH was above 9, the adsorption capacity of LDH decreased (Fig. 11). It can be seen from the potential-pH dependence relationship that when the pH was in the range of 2–5, the zeta potential of MgAl-MMO was completely positive, but the peracid would destroy the layered structure, and the adsorption efficiency would be reduced. In the pH range of 6 to 9, the zeta potential was close to zero, corresponding to higher adsorption efficiency of fluoride ions.[64]

5.2 Temperature

The impact of temperature changes on the fluoride ion removal effect of LDH can be analyzed using the Langmuir and Freundlich isotherm models, which can be used to calculate the
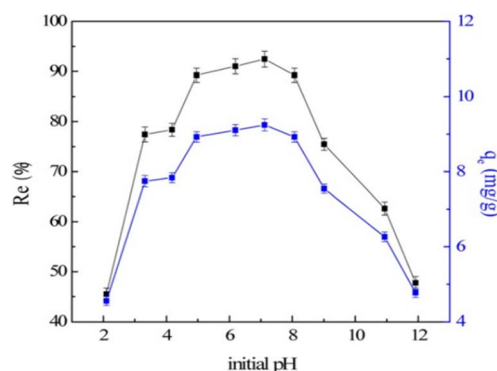

Fig. 11 Effect of initial pH (V = 50 mL, T = 25 ± 1 °C, C0 = 10 mg L^{-1}, R_e is the removal percentage and q_e is the equilibrium adsorption capacity).[64] Copyright 2016, John Wiley and Sons.

Fig. 10 Effect of initial pH on the F$^-$ removal by Ca–Al–CO$_3$ LDH and its modified products. (Initial F$^-$ = 10 mg L^{-1}, adsorbent dose = 1 g L^{-1}, T = 25 ± 1 °C, and q_e is the equilibrium adsorption capacity).[75] Copyright 2020, Elsevier.
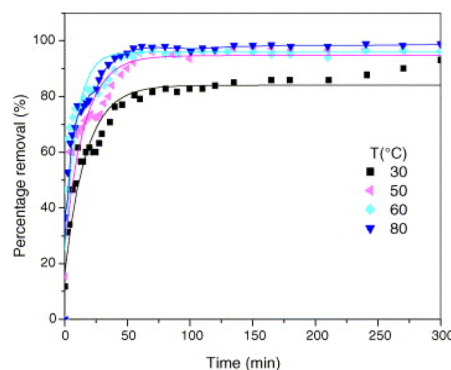

Fig. 12 Relationship between the percentage removal of fluoride ions and the time for various temperatures (V = 1.8 L, pH = 6.0, F$^-$ = 50 mg L^{-1}, and adsorbent mass = 2.0 g).[13] Copyright 2006, Elsevier.

theoretical maximum fluoride removal capacity of LDH. The adsorption mechanism of fluoride ions on the adsorbent surface can also be further determined. By analyzing the pseudo-second-order rate constant of the fluoride ion adsorption reaction of MgAl-MMO at several different temperatures of 30 °C, 40 °C, 50 °C, and 60 °C, it was found that the fluoride ion removal rate increased with temperature (Fig. 12).[13] This phenomenon is explained by the increased active sites of fluoride, which in response increased the interaction of the number of active sites present at the surface of the adsorbent.[64] Some research results on carbonate-type LDH show different trends. For example, the equilibrium adsorption capacity of CO_3^{2-} type CaAl-LDH and MMO derivatives decreased with temperature, indicating that the adsorption of LDH and MMO is an exothermic process.[75,112]

5.3 Dosage

The dosage is the key to efficient and economical utilization of LDH. Generally, as the amount of adsorbent increases, the total number of active sites available for adsorption increases, so the fluoride ion removal efficiency also increases. For example, for carbonate-type CaAl-LDH, when the adsorbent dosage
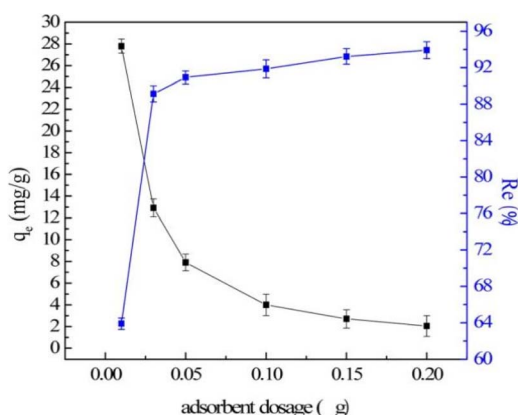

Fig. 13 Effect of adsorbent dosage ($V = 50$ mL; $T = 25 \pm 1$ °C; $C_0 = 10$ mg L; q_e is the equilibrium adsorption capacity).[64] Copyright 2016, John Wiley and Sons.

increased from 0.1 g L^{-1} to 2 g L^{-1}, the removal rate significantly increased from 20% to 90%.[112] However, the equilibrium adsorption capacity of LDH decreased (Fig. 13).[64] This can be explained by the fact that the increase of the LDH adsorbent dosage can lead to incomplete dispersion of particles in the aqueous solution, resulting in the adsorption sites on the adsorbent not being fully exposed and the adsorption of fluoride ions being limited. When the fluoride ion adsorption capacity generated by adding LDH is greater than the total number of fluoride ions in the solution, the equilibrium adsorption capacity will continue to decrease. At this time, it is meaningless to continue to increase the dose of the adsorbent. Therefore, when selecting the adsorbent dose, a comprehensive evaluation should be carried out based on the final removal target of fluoride ions and the cost of the adsorbent. In practice, a certain dosage before reaching the equilibrium adsorption capacity is usually selected, which can ensure better adsorption efficiency and not excessive adsorbent dosage.

5.4 Coexisting anions

The influence of other coexisting anions on the removal of fluoride ions is mainly manifested in the competitive adsorption with fluoride ions.[66,113] By studying the interference effects of sulfate, phosphate, chloride, bromide and nitrate on the adsorption of fluoride ions on MgAl-MMO, it was found that the order of influence of these anions was $PO_4^{3-} > Cl^- \approx SO_4^{2-} > Br^- \gg NO_3^-$ (Fig. 14), mainly because anions with high charge density have a stronger affinity for LDH and are more easily adsorbed; the significant impact of chloride ions may be due to its low molar mass, leading to its molar concentration being higher than that of other anions when the concentration is controlled in mg L^{-1}.[13] In addition, for carbonate CaAl-LDH without thermal activation, the anions such as Cl^-, NO_3^-, SO_4^{2-}, and HCO_3^- have almost no significant impact on the adsorption of fluoride ions.[75]

5.5 Time

Time-dependent adsorption kinetics can provide information on the adsorption rate, adsorption performance, mass transfer
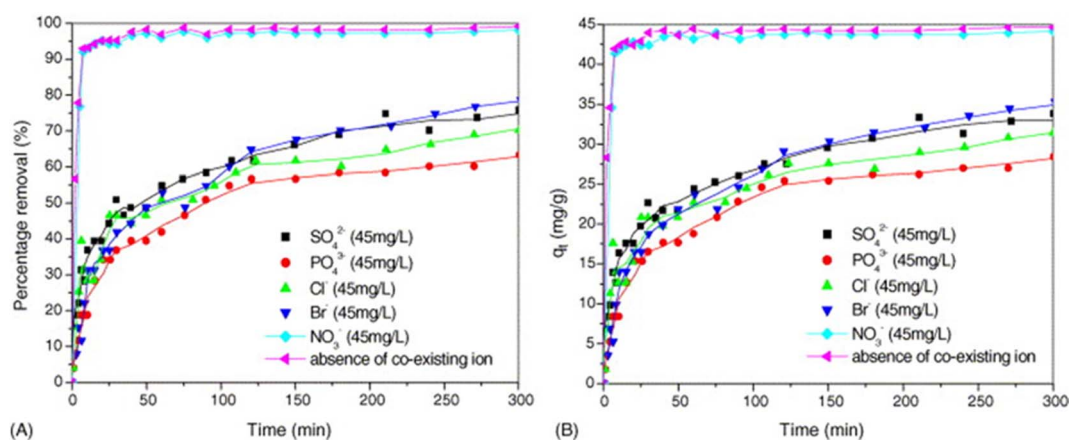

Fig. 14 Relationship between the percentage removal of fluoride and the adsorption time (A) and the adsorption loading of fluoride and the time (B), for various co-existing anions ($V = 1.8$ L, pH = 6.0, F$^-$ = 50 mg L^{-1}, and adsorption mass = 2.0 g).[13] Copyright 2006, Elsevier.

mechanism, *etc.* The adsorption trends of different LDH samples are fast at the beginning and then gradually reach equilibrium, but the specific analysis needs to be fitted with a kinetic model.

Recently, many adsorption kinetic models have been proposed.[114-116] Nevertheless, only a few models have been applied in the fluoride adsorption of LDHs. The pseudo-first-order (PFO)[117] and the pseudo-second-order (PSO)[118] kinetic models are the most widely used in the study of LDH adsorption of fluoride ions; in addition, the Elovich model[119] and the intraparticle diffusion (IP) model[120] are also often used. Both the PFO and PSO models are empirical models. People often summarize the adsorption mechanism that conforms to the PFO model as physical adsorption, and the adsorption mechanism that conforms to the PSO model as chemical adsorption. However, in recent years, some scholars have put forward different views.[114,115] For example, Wang and Guo pointed out that the PFO model is applicable when the initial solute has a high concentration, when there are fewer active sites on the adsorbent and/or in the initial stage of fluoride ion adsorption; meanwhile, the PSO model is applicable when the initial solute has a low concentration, when there are abundant active sites on the adsorbent and/or in the final stage of fluoride ion adsorption.[115] The Elovich model is an empirical model based on heterogeneous surface adsorption, whose fitting effect on the entire adsorption process is usually good.[115] The most commonly used intra-particle diffusion model is the Weber & Morris (W&M) model, which is mainly based on the assumption that intrapore diffusion is the rate-determining step.[105]

According to our statistics (Table 1), the defluorination of most LDH materials is more in line with the PSO kinetic model, indicating that the rate-limiting step of adsorption is the adsorption of surface-active sites in the final stage of fluoride ion adsorption, which may be due to the replacement of divalent ions by trivalent ions in the brucite structure, resulting in a large number of positively charged active sites on the material surface. In the future, more nonlinear regression models can be tried for the fluoride adsorption kinetics of LDH, and the physical meaning can be further clarified. At the same time, more statistical parameters should be used to evaluate the fitting effect.[115]

5.6 Summary

Environmental factors such as pH value, temperature and dosage have basically the same impact on the fluoride removal performance of LDH and MMO materials. The optimal adsorption pH range is between 5 and 8. Too high or too low pH is not conducive to the adsorption of fluoride ions. This is mainly because such a pH range can find the best balance between the structure stabilization of the adsorbent and the competitive adsorption of hydroxide groups. The effect of temperature on LDH and MMO is usually that the adsorption capacity increases as the temperature increases, but different structures may also show abnormal behaviour. The influence of the adsorbent dose is that as the adsorbent dose increases, the fluoride ion removal efficiency gradually reaches equilibrium,

while the adsorption capacity gradually decreases. Therefore, when selecting the adsorbent dose, the cost of the adsorbent and the fluoride ion removal target must be considered comprehensively by determining a certain value before the equilibrium adsorption capacity. The effects of coexisting anions on LDH-based fluoride removal materials are different. The known research reports show that high-valence anions hinder the fluoride removal performance of MMO more than low-valence anions, but have little effect on some intrinsic LDHs. However, this rule is also closely related to the material itself, and more cases may be needed for further verification.

6 Adsorption mechanism

Understanding the adsorption mechanism is the key for the optimization of the fluoride ion adsorption performance of LDH and MMO, and the adsorption mechanism can be indirectly evaluated by fitting the fluoride ion adsorption kinetic model.[121,122] Because LDH and MMO have different structures and surface properties, when classifying and summarizing the adsorption mechanisms, we first summarize the fluoride ion adsorption mechanism of LDH (Section 6.1), and then discuss the adsorption mechanism of LDH-based heterocoagulated composites (Section 6.2), and finally summarize the adsorption mechanism of MMO (Section 6.3). It is worth noting that the adsorption mechanisms obtained by adsorption kinetics analysis (*e.g.*, physical adsorption and chemical adsorption) are macroscopic, while the adsorption mechanisms discussed here are intuitive and at the atomic level. At the end of each microscopic mechanism section, its corresponding macroscopic category is also given.

6.1 Intrinsic adsorption mechanism

6.1.1 Anion exchange. When the affinity between existing interlayer anions and the LDH layer is lower than that between fluoride ions and the LDH layer, such as Cl^- or NO_3^{3-}, fluoride ions can be adsorbed through ion exchange. The fluoride ion removal mechanism of this type of LDH, such as nitrate-based MgCaAl-LDH, is that fluoride ions are first adsorbed on the outer surface and edge of the LDH particles and then are exchanged with NO_3^{3-}, thereby achieving good fluoride ion adsorption (Fig. 15).[38] NiFe-LDH containing Cl^- anions has a similar fluoride removal mechanism.[20] Due to the strong affinity between CO_3^{2-} and the brucite layer, the relevant synthesis or modification should strictly control the environmental atmosphere. Although anion exchange does not change the structure of the brucite layer, it does change the physical phase of LDH including the brucite layer and interlayer anions. Therefore, the anion exchange mechanism is essentially chemical adsorption. In kinetic analysis, anion exchange should conform to the intraparticle diffusion (IP) model (corresponding to interlayer diffusion), but actually, it is found that the rate-controlling step is not IP diffusion but external surface adsorption.[20,38] This contradiction needs to be further clarified.

6.1.2 Cationic complexation. Some metal cations such as Ca, Al, Mg, *etc.* have a greater affinity for fluoride ions. When
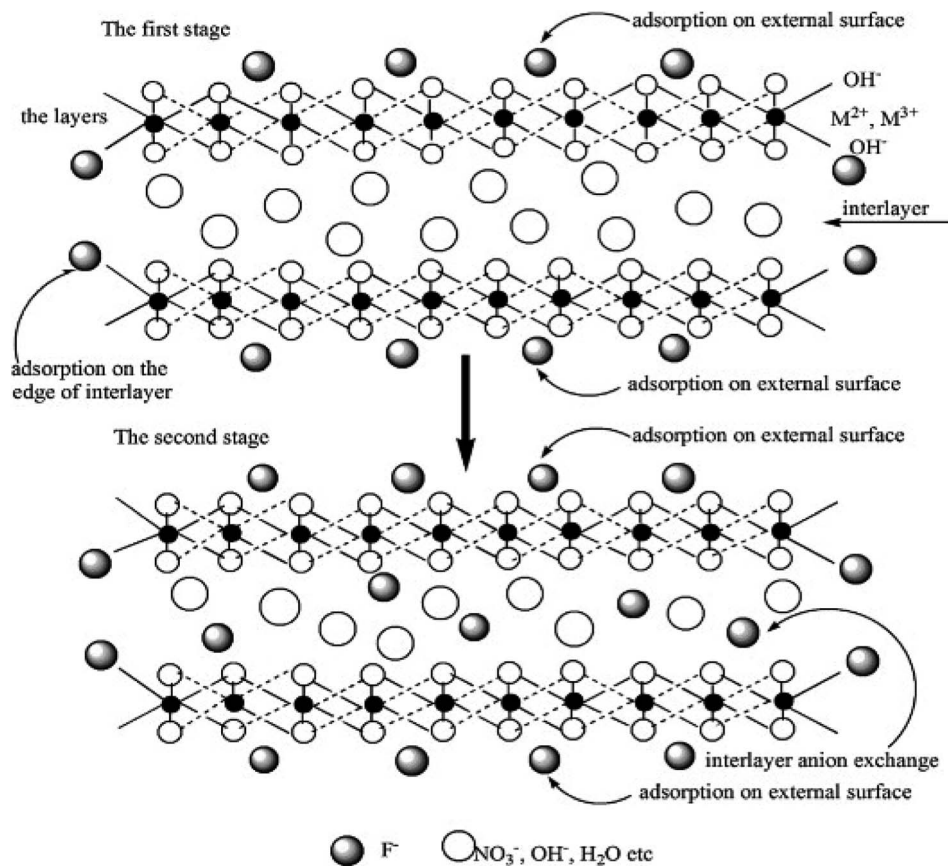
Fig. 15 The anion exchange mechanism for the removal of fluoride ions by $Mg_{2.5}Ca_{0.5}Al-NO_3-LDH$.[38] Copyright 2012, Elsevier.

LDH contains these metal cations, their complexation with fluoride can be used to remove fluoride ions. For example, MgCaFe-LDH will release part of Ca^{2+} during the fluoride ion adsorption process, which will form fluorite. Therefore, the fluoride ion removal mechanism of this type of LDH can be explained by the adsorption of fluoride ions on the surface of LDH and the reaction with Ca^{2+} released from LDH.[40] By studying the metal ion concentration and fluoride ion concentration in solutions at different pH, it was found that carbonate-type CaAl-LDH also has a similar fluoride removal mechanism. Specifically, Al^{3+} leaching from LDH would occur at an alkaline pH of 11.5. At this point, fluoride ions will not complex with metal ions; however, when some acids other than carbonic acid were added to make the solution acidic, fluoride ions would complex with Al^{3+} metal ions to achieve a reduction of fluoride ion concentration. In addition, if CO_2 acidification is used in this process, $CaCO_3$ will be formed, and fluoride ions can be further removed by surface adsorption to this cationic compound (Fig. 16).[112] Cationic complexation is obviously a form of chemical adsorption, and the PSO model usually has a better fitting effect on kinetic analysis.[40,112] However, the explanation of the adsorption mechanism is derived less from the kinetic results and more from the characterization of the adsorbent before and after adsorption and leaching tests.[40,112]

6.1.3 Hydroxyl exchange. The hydroxyl groups in LDH are distributed on the outer and interlayer surfaces. The exchange

between surface hydroxyl groups and fluoride ions is a common adsorption mechanism observed for LDH. However, the exchange of interlayer hydroxyl groups and fluoride ions has not been clearly experimentally proven. The nuclear magnetic resonance (NMR) technique and DFT calculations have been used to study the affinity of MgAl-LDH adsorption sites with fluoride ions at different positions. The results show that the
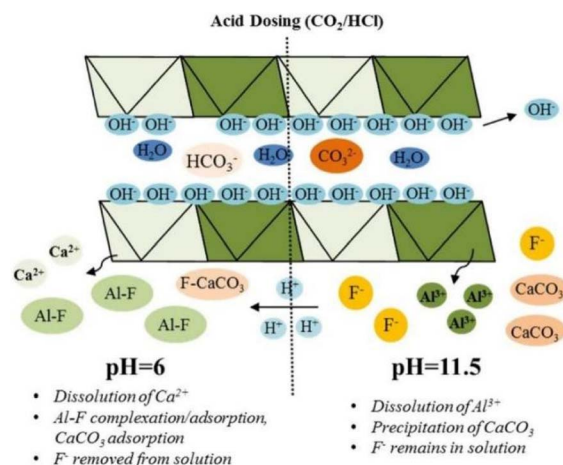

Fig. 16 Cationic complexation mechanism for the removal of fluoride ions by CaAl-LDH.[112] Copyright 2021, Elsevier.

base and edge binding sites of LDH are potential sites for fluoride ion adsorption, but it is difficult to form suitable adsorption sites between layers due to the steric hindrance, electrostatic repulsion, and hydrogen bonding effect of water molecules.[45] Hydroxyl exchange involves the breaking and reconstruction of chemical bonds and therefore belongs to chemical adsorption. The kinetic model involved in this adsorption mechanism is primarily of the active site adsorption type,[115] but the specific physical image is mainly obtained through experimental detection or DFT simulation.[45]

6.1.4   Polar adsorption of the brucite layer. Due to its electropositive nature, the LDH layer directly attracts negatively charged fluoride ions through Coulomb attraction. This process represents physical adsorption. This behavior will exist in any brucite layer in LDH. However, this adsorption process is reversible and unstable and has no selectivity for anions. In the study of LDH fluoride ion removal, replacing divalent metal ions with monovalent metal ions in the LDH layer or increasing the content of trivalent ions in the LDH layer can improve the positive charge density of the LDH layer. In the specific study of fluoride ion removal performance, the fitting of the pseudo-first-order kinetic equation may indirectly give some clues regarding the mechanism for the fluoride ion removal process of LDH. Such studies can be found in the literature.[23,34,87] Polar adsorption of brucite layers is the easiest adsorption mechanism to understand. It is mainly derived from the Coulomb force between the positively charged brucite layer and the negatively charged fluoride ions and belongs to physical adsorption. In kinetic analysis, relevant support can be obtained through an adsorption model with physical significance.[115]
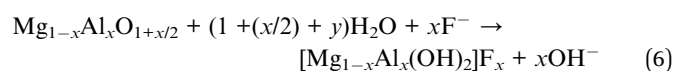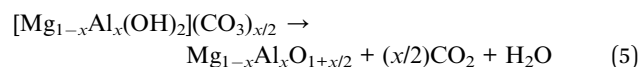
6.2   Heterophase synergy

When LDH is compounded with other materials, the fluoride removal mechanism involves not only the intrinsic adsorption mechanism of LDH, but also the adsorption by the materials compounded with LDH. Therefore, the adsorption mechanism of such materials should be comprehensively considered. For

Fig. 17   Heterophase synergistic mechanism for fluoride ion removal by the Fe$_2$O$_3$@LDH/poly composite.[25] Copyright 2018, Elsevier.

example, the fluoride ion removal mechanism using compounding of cellulose and ZnCe-LDH involves the exchange between fluoride ions and hydroxyl groups on the cellulose surface.[25] The fluoride ion removal mechanism is shown in Fig. 17. When LDH is compounded with some metal oxides, the compounded metal oxides can provide more active sites for the adsorbent, such as non-thermal plasma (NTP) modified CeO$_2$/MgFe-LDH, in which CeO$_2$ was further enhanced by MgFe-LDH's adsorption capacity.[86] The LDH/Al$_2$O$_3$ compounding material with a hierarchical structure prepared by template directional synthesis had a theoretical maximum capacity of 58.7 mg g^{-1} due to the cooperative adsorption of fluoride ions by Al^{3+} in Al$_2$O$_3$ and LDH.[57] Heterophase synergy mainly relies on the adsorption of other phases to improve the defluorination performance or other additional properties of LDH. Different added phases bring about different defluorination mechanisms. Therefore, in the kinetic analysis, it is necessary to combine the added phase type and select an appropriate kinetic model for specific discussion.

6.3   MMO hydration

During the rehydration process of the MMO material, fluoride ions are inserted into the space between LDH layers as interlayer anions. After thermal activation of MgAl-LDH at 500 °C, LDH decomposed into a mixed oxide of magnesium and aluminum (MgAl-MMO). The interlayer carbonate was decomposed and released. When MgAl-MMO was rehydrated, fluoride ions entered the layer as compensating anions.[13] The process is shown in eqn (5) and (6).

$$[Mg_{1-x}Al_x(OH)_2](CO_3)_{x/2} \rightarrow$$
$$Mg_{1-x}Al_xO_{1+x/2} + (x/2)CO_2 + H_2O \quad (5)$$

$$Mg_{1-x}Al_xO_{1+x/2} + (1 +(x/2) + y)H_2O + xF^- \rightarrow$$
$$[Mg_{1-x}Al_x(OH)_2]F_x + xOH^- \quad (6)$$

In addition to entering the structure as interlayer anions during hydration, fluoride ions can also replace some of the hydroxyl groups to achieve the restoration of the brucite-like layered structure. For example, when MgFeLa-MMO co-adsorbed arsenate and fluoride, the addition of La increased the affinity of the brucite layer for fluoride ions. On the one hand, fluoride ions act as interlayer anions to compensate for the charge imbalance of the LDH layer; on the other hand, fluoride ions replace hydroxyl groups to maintain the structural integrity of the brucite layer. In addition, fluoride ions can also be adsorbed on the outer surface of the material.[28] The overall fluoride ion adsorption mechanism is shown in Fig. 18. MgFe-MMO also exhibits a similar fluoride ion adsorption mechanism.[19] However, it must be pointed out that some current studies suggest that fluoride ions are mainly adsorbed on the outer surface of LDH.[123] The current MMO hydration mechanism involves the entry of fluoride ions into the interlayer and the replacement of fluoride ions for hydroxyl groups,[28] which constitutes chemical adsorption. The PSO model is usually better for kinetic analysis, but the adsorption mechanism is mainly obtained through the characterization of the adsorbent
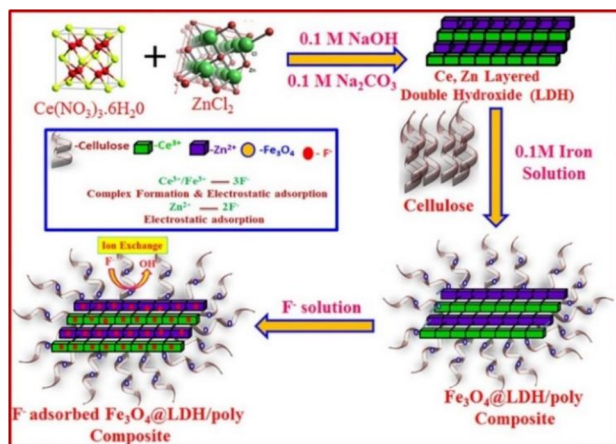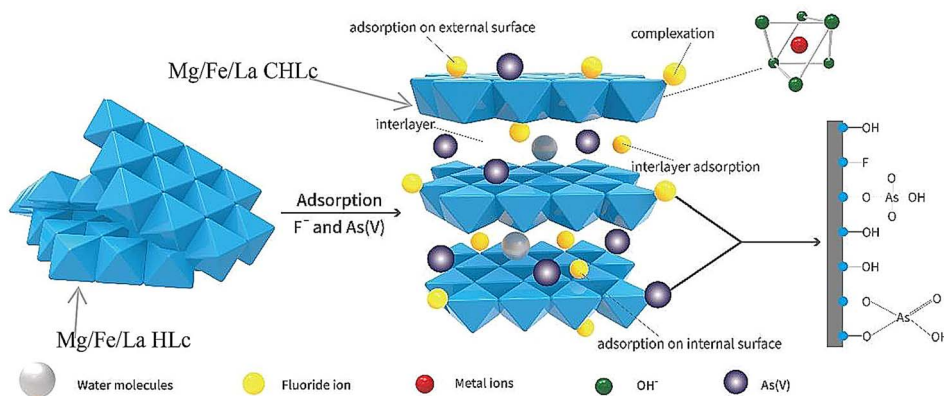
Fig. 18   MMO hydration mechanism for fluoride ion adsorption by MgFeLa-MMO.[28] Copyright 2018, American Chemical Society.

before and after adsorption and DFT simulation,[19,28] because kinetic analysis cannot provide adsorption details.

6.4   Summary

The fluoride ion removal mechanisms of LDH-based adsorbents can be divided into three major categories: intrinsic adsorption, heterophase assisted adsorption, and MMO hydration adsorption. The intrinsic adsorption does not significantly change the brucite layer structure. In this case, LDH interacts with fluoride ions through direct adsorption of lamellar polarity, interlayer anion replacement, partially dissolved cation complexation, and surface hydroxyl exchange. The heterophase assisted adsorption involves the use of the adsorption capacity or dispersion ability of other heterophases. MMO hydration adsorption mainly refers to fluoride ions that are inserted into the interlayer space and replace some of the hydroxyl groups, when MMO is reconstructed to LDH. At present, the adsorption behavior of fluoride ions is mainly studied through kinetic and thermodynamic experiments, assisted by other characterization methods. However, because fluoride ions and hydroxyl groups are similar in nature and ionic radius, most experimental results and characterization methods struggle to provide direct evidence, especially the interlayer hydroxyl exchange mechanism, which requires further investigation. In addition, it should be pointed out that the analysis of adsorption kinetics can only provide some adsorption mechanism information with macroscopic significance, and its connection with the specific microscopic adsorption mechanism needs to be further strengthened.

7.   Conclusion and outlook

This work provides a comprehensive review of the research progress of LDH materials for fluoride ion adsorption in water. The content is arranged according to the logical line of category, synthesis, modification, environmental factors, and adsorption mechanism. Statistical histograms of all LDH studies involved in fluoride removal (that is, including LDH as a component phase and intermediates) are made at the end of each section to show the research hotspot distribution of this field.

Among binary LDHs, LDH composed of aluminum as a trivalent metal is the most studied type of fluoride ion removal LDH with high performance; LDH with Fe as a trivalent metal, which can reduce the risk of Al ion dissolution to a certain extent, shows good fluoride ion removal performance as well, but the number of studies currently is small; LDH with Cr or rare earth elements as a trivalent metal does not show better performance than other binary LDHs, and the cost is higher. Ternary LDHs with/without RE elements show excellent fluoride ion removal performance and large control space over the synthesis parameters, so LDH with multi-metal components is worthy of in-depth study in the future.

Due to the simplicity of the synthesis method, co-precipitation and urea-assisted methods are currently mainly used for the synthesis of LDH original defluorination agents. In comparison, the LDH obtained by the co-precipitation method, which stabilizes the pH value within a smaller range through constant alkali control, has better performance, while the urea method has unique advantages in preparing some special morphologies. Similarly, co-precipitation and urea methods are also the most important synthesis methods of LDH in LDH-based fluoride scavengers (including LDH compounded with other phases and LDH derivatives) and will continue to attract research attention in the future. Although the hydrothermal method can obtain samples with good performance, more experiments are needed to verify it. In addition, the hydrothermal method has higher requirements on equipment than the co-precipitation method, which must be considered in actual production. Microemulsion is an important method for synthesizing monodispersed nanomaterials, but the adsorption capacity of the LDH synthesized in the examples is relatively low, which may be due to the type of material selected. In the future, new LDHs can be synthesized to further verify the effect of this method.

Among the existing modification methods, morphology control is the simplest, but its effect on the fluoride removal is very low; after compounding LDH with other materials, the fluoride ion removal capacity of the material is not high, but the final material may possess new properties that are not observed for raw LDH; after rare earth element doping of LDHs, the

© 2025 The Author(s). Published by the Royal Society of Chemistry

fluoride removal performance is significantly improved compared to the morphology control approach. Acid etching and anion exchange of LDH are the most effective modification methods, but the number of studies is small and further verification is needed. Thermal activation modification is the most studied method, and the fluoride ion removal effect is relatively good, but the balance between energy cost and performance should be considered in future research.

The optimal adsorption pH range of most LDH-based adsorbents is between 5 and 8. A pH that is too high or too low is not conducive to the adsorption of fluoride ions; as the temperature increases, the adsorption capacity of fluoride ions increases, but some structures may show abnormal behavior. As the adsorbent dose increases, the fluoride ion removal rate gradually reaches equilibrium, while the adsorption capacity gradually decreases. The coexisting high-valent anions improve the fluoride removal effect of MMO more than low-valent anions, but have little effect on some intrinsic LDH. The reasons for these inconsistencies need to be analyzed in conjunction with specific materials in the future.

The existing fluoride removal mechanisms of LDH-based adsorbents include intrinsic adsorption, heterophase assisted adsorption and MMO hydration adsorption. Intrinsic adsorption does not significantly change the structure of the brucite-like layer, mainly through lamellar polarity, interlayer anion exchange, complexation of partially dissolved cations, surface hydroxyl exchange, *etc.* Heterophase assisted adsorption utilizes the adsorption capacity or dispersion capacity of other phases; MMO hydration adsorption mainly utilizes the memory effect in the recovery process of the LDH structure. At present, there are still few detailed studies on each adsorption mechanism, and direct evidence is still lacking.

Therefore, through a summary of previous research, several key points for future research on LDH-based adsorbents are proposed: (1) to synthesize high-efficiency fluoride-removing LDH by optimizing the ratio of multi-metallic components; (2) use the hydrothermal or microemulsion method to synthesize different LDH nanomaterials to further verify the effect of these methods; (3) further test the modification effect of acid etching; (4) develop a low-cost modification process and expand the application scope of LDH, such as using multiple modification processes to jointly improve the fluoride removal performance of LDH and study the possible synergistic effects between different modification methods; (5) conduct targeted analysis on the influence of environmental factors that are inconsistent with the general rules, based on the structure and morphological characteristics of LDH itself; (6) use more new methods such as *in situ* observation and computer simulation[76] to further reveal the microscopic mechanism of LDH defluorination; (7) study the chemical stability of LDH structures during fluoride adsorption to prevent the release of harmful ions into treated water and wastewater; (8) in addition, due to the needs of sustainable development of human society, special attention should be paid to the recycling of LDH in future research. Through these efforts, it is expected that fluoride ion adsorption materials can be developed with low cost, a good fluoride removal effect, low secondary pollution, and easy recycling.

Data availability

This review is based on the existing research and literature. No primary research results, software or code have been included and no new data were generated or analysed as part of this review.

Author contributions

Conflicts of interest

There are no conflicts to declare.

Acknowledgements

Notes and references

1 R. Sauerheber, *J. Environ. Public Health*, 2013, **2013**, 439490–439502.

2 D. Khandare and S. Mukherjee, *Mater. Today: Proc.*, 2019, **18**, 1146–1155.

3 G. Mishra, B. Dash and S. Pandey, *Appl. Clay Sci.*, 2018, **153**, 172–186.

4 G. R. Williams and D. O'Hare, *J. Mater. Chem.*, 2006, **16**, 3065–3074.

5 K. Li, G. Wang, D. Li, Y. Lin and X. Duan, *Chin. J. Chem. Eng.*, 2013, **21**, 453–462.

6 K. L. Erickson, T. E. Bostrom and R. L. Frost, *Mater. Lett.*, 2005, **59**, 226–229.

7 P. S. Jijoe, S. R. Yashas and H. P. Shivaraju, *Environ. Chem. Lett.*, 2021, **19**, 2643–2661.

8 L. R. de Carvalho Costa, I. V. Jurado-Davila, J. T. D. Oliveira, K. G. P. Nunes, D. C. Estumano, R. A. de Oliveira, E. Carissimi and L. A. Féris, *Appl. Sci.*, 2024, **14**(5), 2161.

9 C. Onyutha, E. Okello, R. Atukwase, P. Nduhukiire, M. Ecodu and J. N. Kwiringira, *Sustainable Environ. Res.*, 2024, **34**(1), 1–15.

10 A. R. Gupta, V. C. Joshi and S. Sharma, *Advances in Drinking Water Purification*, 2024, pp. 181–200.

11 S. Shan, Y. Zhang, S. Q. Shi and C. Xia, *Environ. Sci.: Water Res. Technol.*, 2024, **10**, 1034–1060.

12 N. A. Tajuddin, E. F. B. Sokeri, N. A. Kamal and M. Dib, *J. Environ. Chem. Eng.*, 2023, **11**, 110305.

13 L. Lv, J. He, M. Wei, D. G. Evans and X. Duan, *J. Hazard. Mater.*, 2006, **133**, 119–128.

14 Z. Sun, J.-S. Park, D. Kim, C.-H. Shin, W. Zhang, R. Wang and P. Rao, *Water, Air, Soil Pollut.*, 2016, **228**, 23–29.

15 X. Zhao, L. Zhang, P. Xiong, W. Ma, N. Qian and W. Lu, *Microporous Mesoporous Mater.*, 2015, **201**, 91–98.

16 Y. Li, R. Narducci, A. Varone, S. Kaciulis, E. Bolli and R. Pizzoferrato, *Processes*, 2021, **9**, 2109–2126.

17 T. Zhang, Q. Li, H. Xiao, H. Lu and Y. Zhou, *Ind. Eng. Chem. Res.*, 2012, **51**, 11490–11498.

18 T. Wu, L. Mao and H. Wang, *RSC Adv.*, 2015, **5**, 23246–23254.

19 D. Kang, X. Yu, S. Tong, M. Ge, J. Zuo, C. Cao and W. Song, *Chem. Eng. J.*, 2013, **228**, 731–740.

20 M. Tipplook, T. Sudare, H. Shiiba, A. Seki and K. Teshima, *ACS Appl. Mater. Interfaces*, 2021, **13**, 51186–51197.

21 S. Ziegenheim, G. Varga, M. Szabados, P. Sipos and I. Pálinkó, *Chem. Pap.*, 2017, **72**, 897–902.

22 P. Koilraj and S. Kannan, *Chem. Eng. J.*, 2013, **234**, 406–415.

23 S. Mandal, S. Tripathy, T. Padhi, M. K. Sahu and R. K. Patel, *J. Environ. Sci.*, 2013, **25**, 993–1000.

24 L. Kong, Y. Tian, Z. Pang, X. Huang, M. Li, N. Li, J. Zhang, W. Zuo and J. Li, *Chem. Eng. J.*, 2020, **382**, 122963–122974.

25 N. Ammavasi and R. Mariappan, *J. Environ. Chem. Eng.*, 2018, **6**, 5645–5654.

26 L. Kong, Y. Tian, Z. Pang, X. Huang, M. Li, R. Yang, N. Li, J. Zhang and W. Zuo, *Chem. Eng. J.*, 2019, **371**, 893–902.

27 S. Luo, Y. Guo, Y. Yang, X. Zhou, L. Peng, X. Wu and Q. Zeng, *J. Solid State Chem.*, 2019, **275**, 197–205.

28 P. Wu, L. Xia, Y. Liu, J. Wu, Q. Chen and S. Song, *ACS Sustain. Chem. Eng.*, 2018, **6**, 16287–16297.

29 P. Wu, J. Wu, L. Xia, Y. Liu, L. Xu and S. Song, *RSC Adv.*, 2017, **7**, 26104–26112.

30 T. Mak Yu, A. Caroline Reis Meira, J. Cristina Kreutz, L. Effting, R. Mello Giona, R. Gervasoni, A. Amado de Moura, F. Maestá Bezerra and A. Bail, *Appl. Surf. Sci.*, 2019, **467–468**, 1195–1203.

31 J. Cai, X. Zhao, Y. Zhang, Q. Zhang and B. Pan, *J. Colloid Interface Sci.*, 2018, **509**, 353–359.

32 Z. Jia, S. Hao and X. Lu, *J. Environ. Sci.*, 2018, **70**, 63–73.

33 E. Dore and F. Frau, *J. Water Proc. Eng.*, 2019, **31**, 100864.

34 W. Ma, N. Zhao, G. Yang, L. Tian and R. Wang, *Desalination*, 2011, **268**, 20–26.

35 Y. B. Pu, J. R. Wang, H. Zheng, P. Cai and S. Y. Wu, *Adv. Mater. Res.*, 2013, **681**, 21–25.

36 X.-R. Ma, X.-Y. Wei, R. Dang, W. Guo, Y.-H. Kang, X. Li, Y. Gao, J.-J. Bai, Y. Zhang, Z.-F. Zhang, Y.-J. Ma and Z.-M. Zong, *Appl. Clay Sci.*, 2021, **211**, 106191–106202.

37 M. A. Teixeira, A. B. Mageste, A. Dias, L. S. Virtuoso and K. P. F. Siqueira, *J. Clean. Prod.*, 2018, **171**, 275–284.

38 T. Lv, W. Ma, G. Xin, R. Wang, J. Xu, D. Liu, F. Liu and D. Pan, *J. Hazard. Mater.*, 2012, **237–238**, 121–132.

39 W. Ma, T. Lv, X. Song, Z. Cheng, S. Duan, G. Xin, F. Liu and D. Pan, *J. Hazard. Mater.*, 2014, **268**, 166–176.

40 W. Ma, Y. Chen, W. Zhang and W. Zhao, *J. Fluorine Chem.*, 2017, **200**, 153–161.

41 L. A. Ramírez-Llamas, R. Leyva-Ramos, A. Jacobo-Azuara, J. M. Martínez-Rosales and E. D. Isaacs-Páez, *Adsorpt. Sci. Technol.*, 2015, **33**, 393–410.

42 M. Dessalegne, F. Zewge, N. Pfenninger, C. A. Johnson and I. Diaz, *Water, Air, Soil Pollut.*, 2016, **227**, 381–393.

43 L. Lv, J. He, M. Wei, D. G. Evans and Z. Zhou, *Water Res.*, 2007, **41**, 1534–1542.

44 P.-P. Huang, C.-Y. Cao, F. Wei, Y.-B. Sun and W.-G. Song, *RSC Adv.*, 2015, **5**, 10412–10417.

45 C. Ren, M. Zhou, Z. Liu, L. Liang, X. Li, X. Lu, H. Wang, J. Ji, L. Peng, G. Hou and W. Li, *Environ. Sci. Technol.*, 2021, **55**, 15082–15089.

46 P. Cai, H. Zheng, P. Liang and S. P. Liang, *Adv. Mater. Res.*, 2010, **160–162**, 182–188.

47 T. Kameda, J. Oba and T. Yoshioka, *J. Environ. Manage.*, 2017, **188**, 58–63.

48 T. Kameda, J. Oba and T. Yoshioka, *J. Hazard. Mater.*, 2015, **300**, 475–482.

49 J. Liu, X. Yue, X. Lu and Y. Guo, *Water*, 2018, **10**, 745–755.

50 G. K. Sarma and M. H. Rashid, *J. Chem. Eng. Data*, 2018, **63**, 2957–2965.

51 Q. Chang, L. Zhu, Z. Luo, M. Lei, S. Zhang and H. Tang, *Ultrason. Sonochem.*, 2011, **18**, 553–561.

52 S. Moriyama, K. Sasaki and T. Hirajima, *Appl. Clay Sci.*, 2016, **132–133**, 460–467.

53 A. S. Garzón-Pérez, S. P. Paredes-Carrera, L. F. Flores-Carlos, N. V. Arteaga-Larios, H. Martínez-Gutiérrez and I. Rodríguez-Torres, *J. Dispersion Sci. Technol.*, 2023, 1–15.

54 L. Batistella, L. D. Venquiaruto, M. Di Luccio, J. V. Oliveira, S. B. C. Pergher, M. A. Mazutti, D. de Oliveira, A. J. Mossi, H. Treichel and R. Dallago, *Ind. Eng. Chem. Res.*, 2011, **50**, 6871–6876.

55 N. A. Oladoja, Y. Liu, J. E. Drewes and B. Helmreich, *Chem. Eng. J.*, 2016, **283**, 1154–1167.

56 L. Mao, T. Wu and H. Wang, *Desalination Water Treat.*, 2014, **56**(11), 3067–3074.

57 T. Zhang, H. Yu, Y. Zhou, J. Rong, Z. Mei and F. Qiu, *Korean J. Chem. Eng.*, 2015, **33**, 720–725.

58 T. Zhang, B. Zhao, Q. Chen, X. Peng, D. Yang and F. Qiu, *Appl. Biol. Chem.*, 2019, **62**, 12–18.

59 S. Chen, Y. Xu, Y. Tang, W. Chen, S. Chen, L. Hu and G. Boulon, *RSC Adv.*, 2020, **10**, 44361–44372.

60 C. Gao, X.-Y. Yu, T. Luo, Y. Jia, B. Sun, J.-H. Liu and X.-J. Huang, *J. Mater. Chem. A*, 2014, **2**, 2119–2128.

61 K. Pandi, S. Periyasamy and N. Viswanathan, *Int. J. Biol. Macromol.*, 2017, **104**, 1569–1577.

62 F. Li, J. Jin, Z. Shen, H. Ji, M. Yang and Y. Yin, *J. Hazard. Mater.*, 2020, **388**, 121734–121746.

63 H. Wang, J. Chen, Y. Cai, J. Ji, L. Liu and H. H. Teng, *Appl. Clay Sci.*, 2007, **35**, 59–66.

64 L. Bo, Q. Li, Y. Wang, L. Gao, X. Hu and J. Yang, *Environ. Prog. Sustain. Energy*, 2016, **35**, 1420–1429.

65 D. Wan, Y. Liu, S. Xiao, J. Chen and J. Zhang, *Colloids Surf., A*, 2015, **469**, 307–314.

66 P. Cai, H. Zheng, C. Wang, H. Ma, J. Hu, Y. Pu and P. Liang, *J. Hazard. Mater.*, 2012, **213–214**, 100–108.

67 S. Moriyama, K. Sasaki and T. Hirajima, *Chemosphere*, 2014, **95**, 597–603.

68 S.-B. Kim, S.-Y. Yoon, J.-K. Kang, J.-A. Park, C.-G. Lee and J.-H. Kim, *Water Supply*, 2013, **13**, 249–256.

69 J. Liu, L. Xie, X. Yue, C. Xu and X. Lu, *Int. J. Environ. Sci. Technol.*, 2019, **17**, 673–682.

70 S. S. Ravuru, A. Jana and S. De, *Sep. Purif. Technol.*, 2021, **277**, 119631–119645.

71 D. Chen, Y. Yu, P. Cheng, Y. Arbid, H. Liu, X. Zou and T. Chen, *J. Environ. Eng.*, 2023, **149**(1), 04022090.

72 H. Bessaies, S. Iftekhar, M. B. Asif, J. Kheriji, C. Necibi, M. Sillanpaa and B. Hamrouni, *J. Environ. Sci.*, 2021, **102**, 301–315.

73 P. S. Ghosal and A. K. Gupta, *RSC Adv.*, 2015, **5**, 105889–105900.

74 P. S. Ghosal, A. K. Gupta and S. Ayoob, *Appl. Clay Sci.*, 2015, **116–117**, 120–128.

75 L. Wei, F. Zietzschmann, L. C. Rietveld and D. van Halem, *Chemosphere*, 2020, **243**, 125307–125314.

76 F. Liu, L. Wan, H. Wang, C. Zhong, X. Min and L. Zhang, *Chem. Eng. J.*, 2023, **452**, 139400.

77 M. L. Jiménez-Núñez, M. T. Olguín and M. Solache-Ríos, *Sep. Sci. Technol.*, 2007, **42**, 3623–3639.

78 S. Mandal and S. Mayadevi, *J. Hazard. Mater.*, 2009, **167**, 873–878.

79 S. Mandal and S. Mayadevi, *Appl. Clay Sci.*, 2008, **40**, 54–62.

80 S. Mandal and S. Mayadevi, *Chemosphere*, 2008, **72**, 995–998.

81 O. Saber, S. M. Asiri, M. F. Ezzeldin, W. I. M. El-Azab and M. Abu-Abdeen, *Materials*, 2020, **13**, 2524.

82 S. Mayadevi, M. D. Kirandas, A. M. Manilal and S. Mandal, *Indian J. Chem. Technol.*, 2024, **31**(1), 152–161.

83 J. Cai, Y. Zhang, B. Pan, W. Zhang, L. Lu and Q. Zhang, *Water Res.*, 2016, **102**, 109–116.

84 J. Zhou, Y. Cheng, J. Yu and G. Liu, *J. Mater. Chem.*, 2011, **21**, 19353–19361.

85 K. Li, H. Liu, S. Li, Q. Li, S. Li and Q. Wang, *J. Environ. Sci.*, 2023, **126**, 153–162.

86 T. Zhang, Q. Li, H. Xiao, Z. Mei, H. Lu and Y. Zhou, *Appl. Clay Sci.*, 2013, **72**, 117–123.

87 H. Wu, H. Zhang, Q. Yang, D. Wang, W. Zhang and X. Yang, *Materials*, 2017, **10**, 1320–1337.

88 M. E. Mahmoud, G. F. El-Said, A. A. S. Elnashar and G. A. A. Ibrahim, *J. Ind. Eng. Chem.*, 2024, **133**, 561–576.

89 Z. Li, S. Zheng, J. Yan, P. Qian and S. Ye, *Chem. Eng. J.*, 2024, **480**, 147950.

90 J. Cai, Y. Zhang, Y. Qian, C. Shan and B. Pan, *Sci. Rep.*, 2018, **8**, 11741–11751.

91 A. N. Wagassa, T. A. Shifa, A. Bansiwal and E. A. Zereffa, *Environ. Sci. Pollut. Res. Int.*, 2023a, **30**(56), 119084–119094.

92 D. Bao, H. Wang, W. Liao and H.-Q. Li, *Environ. Eng. Sci.*, 2020, **37**, 623–636.

93 T. Huiyuan, L. Yang, X. Mengyan, C. Baoyu, L. Chang, D. Xiuhong, W. Zehua, D. Xianying and C. Jiehu, *Arab. J. Chem.*, 2024, **17**(3), 105645.

94 A. N. Wagassa, L. T. Tufa, J. Lee, E. A. Zereffa and T. A. Shifa, *Glob. Chall.*, 2023, **7**(6), 2300018.

95 M. Yoshimura and K. Byrappa, *J. Mater. Sci.*, 2007, **43**, 2085–2103.

96 L. Ai, C. Zhang and L. Meng, *J. Chem. Eng. Data*, 2011, **56**, 4217–4225.

97 J.-M. Oh, S.-H. Hwang and J.-H. Choy, *Solid State Ionics*, 2002, **151**, 285–291.

98 X. Zhi Ping and L. Guo Qing (Max), *Chem. Mater.*, 2005, **17**, 1055–1062.

99 X. Zhi Ping and L. Guo Qing (Max), *Chem. Mater.*, 2005, **17**, 1055–1062.

100 F. L. Theiss, G. A. Ayoko and R. L. Frost, *Appl. Surf. Sci.*, 2016, **383**, 200–213.

101 J. He, M. Wei, B. Li, Y. Kang, D. G. Evans and X. Duan, *Layered Double Hydroxides*, 2006, vol. 119, pp. 89–119.

102 M. V. Bukhtiyarova, *J. Solid State Chem.*, 2019, **269**, 494–506.

103 Z. Liu, R. Ma, Y. Ebina, N. Iyi, K. Takada and T. Sasak, *Langmuir*, 2007, **23**, 861–867.

104 M. Adachi-Pagano, C. Forano and J.-P. Besse, *J. Mater. Chem.*, 2003, **13**, 1988–1993.

105 L. Zhang, X. Qiu and J. Chen, *J. Water Proc. Eng.*, 2019, **32**, 100987–100996.

106 T. Sudare, M. Dubois, N. Louvain, M. Kiyama, F. Hayashi and K. Teshima, *Inorg. Chem.*, 2020, **59**, 1602–1610.

107 Y.-F. Lung, Y.-F. Syu, M.-C. Lin and J.-Y. Uan, *RSC Adv.*, 2014, **4**, 57646–57657.

108 B.-K. Kim, G.-H. Gwak, T. Okada and J.-M. Oh, *J. Solid State Chem.*, 2018, **263**, 60–64.

109 L. Lv, *Desalination*, 2007, **208**, 125–133.

110 L. Lv, *J. Water Supply: Res. Technol.–AQUA*, 2006, **55**, 413–418.

111 M. L. Jiménez-Núñez, M. Solache-Ríos and M. T. Olguín, *Sep. Sci. Technol.*, 2010, **45**, 786–793.

112 L. Wei, F. Zietzschmann, L. C. Rietveld and D. van Halem, *J. Water Proc. Eng.*, 2021, **40**, 101957–101963.

113 F. Delorme, A. Seron, A. Gautier and C. Crouzet, *J. Mater. Sci.*, 2007, **42**, 5799–5804.

114 G. W. Kajjumba, S. Emik, A. Öngen, H. K. Özcan and S. Aydın, *Advanced Sorption Process Applications*, 2018, pp. 1–19.

115 J. Wang and X. Guo, *J. Hazard Mater.*, 2020, **390**, 122156.

116 H. Qiu, L. Lv, B. C. Pan, Q. L. Zhang, W. M. Zhang and Q. X. Zhang, *J. Zhejiang Univ., Sci., A*, 2009, **10**(5), 716–724.

117 S. Lagergren and K. Sven, *Vetenskapsakad. Handl.*, 1898, **24**, 1–39.

118 Y. S. Ho, D. A. J. Wase and C. F. Forster, *Water SA*, 1996, **22**, 219–224.

119 S. Y. Elovich and O. G. Larinov, *Izv. Akad. Nauk SSSR, Otd. Khim. Nauk*, 1962, **2**, 209–216.

120 W. J. Weber and J. C. Morris, *ASCE Sanit. Eng. Div. J.*, 1963, **1**, 1–2.

121 L. Lv, J. He, M. Wei and X. Duan, *Ind. Eng. Chem. Res.*, 2006, **45**, 8623–8628.

122 T. Kameda, J. Oba and T. Yoshioka, *J. Environ. Manage.*, 2015, **156**, 252–256.

123 F. L. Theiss, G. A. Ayoko and R. L. Frost, *J. Therm. Anal. Calorim.*, 2012, **112**, 649–657.